

Development of Multi-Walled Carbon Nanotube-Based Flexible Screen- Printed Disposable Electrodes for Sensor Applications

Submitted to the Graduate School of Natural and Applied Sciences
in partial fulfillment of the requirements for the degree of

Master of Science

in Biomedical Engineering

by

Merve Oğuz

ORCID 0000-0002-7999-0005

July, 2023

This is to certify that we have read the thesis **Development of Multi-Walled Carbon Nanotube-Based Flexible Screen-Printed Disposable Electrodes for Sensor Applications** submitted by **Merve Oğuz**, and it has been judged to be successful, in scope and in quality, at the defense exam and accepted by our jury as a MASTER'S THESIS.

APPROVED BY:

Advisor: **Assoc. Prof. Dr. Mustafa Şen**
İzmir Kâtip Çelebi University

Committee Members:

Assoc. Prof. Dr. Nermin AVŞAR TOPALOĞLU
İzmir Kâtip Çelebi University

Assoc. Prof. Dr. İlker POLATOĞLU
Masisa Celal Bayar University

Date of Defense: July 31, 2023

Declaration of Authorship

I, **Merve Oğuz**, declare that this thesis titled **Development of Multi-Walled Carbon Nanotube-Based Flexible Screen-Printed Disposable Electrodes for Sensor Applications** and the work presented in it are my own. I confirm that:

- This work was done wholly or mainly while in candidature for the Master's / Doctoral degree at this university.
- Where any part of this thesis has previously been submitted for a degree or any other qualification at this university or any other institution, this has been clearly stated.
- Where I have consulted the published work of others, this is always clearly attributed.
- Where I have quoted from the work of others, the source is always given. This thesis is entirely my own work, with the exception of such quotations.
- I have acknowledged all major sources of assistance.
- Where the thesis is based on work done by myself jointly with others, I have made clear exactly what was done by others and what I have contributed myself.

Date: 31.07.2023

Development of Multi-Walled Carbon Nanotube-Based Flexible Screen-Printed Disposable Electrodes for Sensor Applications

Abstract

Millions of people worldwide suffer from diabetes and diseases caused by diabetes. As a result of the statistical studies carried out by the World Health Organization (WHO), the number of people suffering from diabetes was 108 million in 1980, then it was increased to 422 million in 2014. Diabetes is increasing rapidly, particularly in underdeveloped and developing countries and it was predicted that 1.5 million people died because of it only in 2019 (WHO, 2021). There are various life-threatening diseases that can be caused by diabetes, such as kidney failure, amputation of the lower limbs, blindness, stroke and myocardial infarction [1]. In this context, it is important to measure glucose levels. Here, a flexible, low-cost, disposable, quite selective and sensitive MWCNT-based SPE was fabricated for detection of dopamine and sweat glucose. A novel conductive paste formulation composed of acrylic varnish and MWCNT was prepared and optimized for printing SPEs using a computer numerical control (CNC)-made stencil. The electrodes were electrochemically characterized and subjected to physical stress to investigate their mechanical durability in extreme situations such as heavy exercise. Reproducibility of the production approach and the stability of the produced electrodes were also demonstrated. The electrochemical performance of the electrodes were tested with first dopamine and then glucose. The SPE displayed a low limit of detection (LOD) with a linear response. MWCNTs and its micro-/nano-porous network morphology observed in scanning electron

microscope (SEM) provided a large surface-to-volume ratio, which potentially contributed to high sensitivity. Detection of glucose was carried out based on electrochemical-enzymatic redox cycling in artificial sweat; wherein the flexible SPE-based biosensor exhibited a linear response with a low LOD and good sensitivity. Overall, the results clearly showed that SPEs had an excellent electrochemical behavior and are expected to contribute to wearable sensor technology due to their stability, sensitivity and flexible nature.

Keywords: Screen-printed electrodes, multi-walled carbon nanotubes, dopamine, glucose, flexible biosensors

Sensör Uygulamaları İçin Çok Duvarlı Karbon Nanotüp Tabanlı Esnek Ekran Baskılı Tek Kullanımlık Elektrotların Geliştirilmesi

ÖZ

Dünya çapında milyonlarca insan diyabet ve diyabetin neden olduğu hastalıklardan muzdariptir. Dünya Sağlık Örgütü'nün (WHO) yaptığı istatistiksel çalışmalar sonucunda 1980'de 108 milyon olan diyabet hastası sayısı 2014'te 422 milyona yükselmiştir. Diyabet, özellikle de düşük ve orta gelirli ülkelerde hızla artmaktadır ve sadece 2019 yılında 1,5 milyon kişinin bu nedenle öldüğü tahmin edilmektedir (WHO, 2021). Diyabetin neden olabileceği böbrek yetmezliği, alt uzuvların amputasyonu, körlük, inme ve miyokard enfarktüsü gibi hayatı tehdit eden çeşitli hastalıklar vardır [1]. Bu bağlamda, glikoz seviyelerinin ölçülmesi önemlidir. Burada, dopamin (DA) ve ter glikozunun tespiti için esnek, düşük maliyetli, tek kullanımlık, oldukça seçici ve hassas çok duvarlı karbon nanotüp (MWCNT) tabanlı ekran baskılı elektrot (SPE) geliştirilmiştir. Akrilik vernik ve MWCNT'den oluşan yeni bir iletken macun formülasyonu hazırlanmıştır ve bilgisayarlı sayısal kontrol (CNC) yapımı bir şablon kullanılarak SPE'leri basmak için optimize edilmiştir. Elektrotlar, ağır egzersiz gibi aşırı durumlarda mekanik dayanıklılıklarını araştırmak için elektrokimyasal olarak karakterize edilmiştir ve fiziksel strese tabi tutulmuştur. Üretim yaklaşımının tekrar üretilebilirliği ve üretilen elektrotların kararlılığı da gösterilmiştir. Elektrotların elektrokimyasal performansı önce DA ve ardından glikoz ile test edilmiştir. SPE, doğrusal bir yanıtla birlikte düşük tespit limiti (LOD) ile göstermiştir. Taramalı elektron mikroskopunda (SEM) gözlemlenen MWCNT'ler ve mikro-/nano-gözenekli ağ morfolojisi, potansiyel olarak yüksek hassasiyete katkıda bulunan geniş bir yüzey-hacim oranı sağladı. Yapay terde elektrokimyasal-enzimatik redoks döngüsüne dayalı

olarak glikoz tespiti yapılmıştır; burada esnek SPE tabanlı biyosensör, düşük bir LOD ve iyi bir hassasiyet ile doğrusal bir tepki sergilemiştir. Genel olarak sonuçlar, SPE'lerin mükemmel elektrokimyasal davranışa sahip olduğunu ve kararlılıkları, hassasiyetleri ve esnek yapıları nedeniyle giyilebilir sensör teknolojisine katkıda bulunmalarının beklendiğini açıkça göstermiştir.

Anahtar Kelimeler: Ekran baskı elektrotlar, çok-duvarlı karbon nanotüpler, dopamin, glukoz, esnek biyosensörler

To my family

Acknowledgment

Firstly, I want to express my sincere gratitude to my advisor, Assoc. Prof. Dr. Mustafa Şen for his precious advice, continuous support, great help, patience, and guidance during my MSc education. His deep knowledge and abundant experience have encouraged me throughout my academic research and daily life.

I specially thank İpek Avcı and Elif Yüzer for their friendliness, patience to me, collaboration and endless help during the experiments. It was an honor for me to work with them.

I am so thankful to Deniz Hande Kısa, Gülşah Sunal, Tuğba Akkaş and Emine Hilal Altıntop for their help, support and friendship.

I would also like to express my gratitude to Elif Nur Bilgin, who never spared her support, love and beautiful energy even though she is miles away.

I would like to express my deepest love to my family, who offered me different perspectives, always stood by me and supported me, and showed endless patience.

I would like to thank my aunt Menekşe Telci and her family, who opened her house and supported me when I needed it most.

Finally, I would like to thank the The Scientific and Technological Research Council of Turkey (TUBITAK), for providing the funding which allowed me to undertake this research. This study was financially supported by TUBITAK, 2210/C- Domestic Priority Areas Graduate Scholarship Program (Application No: 1649B022111832).

Table of Contents

Declaration of Authorship	ii
Abstract	iii
Öz	v
Acknowledgment	viii
List of Figures	xi
List of Tables.....	xiii
List of Abbreviations.....	xiv
List of Symbols	xix
1 Introduction	1
1.1 Screen Printing.....	1
1.1.1 Screen Printed Electrodes (SPE)	3
1.1.2 Screen Printed Carbon Electrodes (SPCE)	5
1.2 Carbon Nanomaterials	6
1.2.1 Multi-Walled Carbon Nanotubes (MWCNT)	8
1.2.2 MWCNT Production Techniques	11
1.2.3 MWCNT-Based SPCE Biosensors.....	15
1.3 Enzyme Biosensors	18
1.4 Dopamine.....	21
1.4.1 Importance of Dopamine	21
1.4.2 Dopamine Detection	22
1.5 Glucose	24
1.5.1 Glucose Metabolism.....	24

1.5.2	Importance of Glucose Detection.....	26
1.5.3	Methods for Glucose Detection.....	27
1.6	Aim of The Study.....	30
2	Material and Method	32
2.1	Materials	32
2.2	Fabrication of MWCNT-Based SPCEs by Screen Printing Method	33
2.3	Electrochemical Characterization	34
2.4	Dopamine Detection	35
2.5	SPCE-Based Glucose Biosensor.....	36
2.6	Selectivity Test.....	37
2.7	Cytotoxicity.....	37
3	Results and Discussion	39
3.1	Fabrication of MWCNT-Based SPCE.....	39
3.2	Surface Characterization	43
3.3	Dopamine Detection	44
3.4	SPCE-Based Glucose Biosensor.....	45
3.5	Selectivity Test.....	48
3.6	Cytotoxicity.....	49
4	Conclusion.....	51
	References	52
	Appendices.....	70
	Appendix A Publications from the Thesis.....	71
	Curriculum Vitae	72

List of Figures

Figure 1.1: Schematic of the screen-printing system.....	1
Figure 1.2: Structure of multi-walled carbon nanotubes, representing σ - and π -covalent bonds	8
Figure 1.3: Types of the chirality of the SWCNTs (a), and honeycomb shape of graphene layer with the chirality (b)	9
Figure 1.4: Schematic of arc discharge chamber for production of CNTs	12
Figure 1.5: Schematic of laser ablation chamber for production of CNTs	13
Figure 1.6: Schematic of chemical vapor deposition for production of CNTs	14
Figure 1.7: Schematic of enzyme immobilization techniques	19
Figure 1.8: Pathways for synthesis of dopamine, serotonin, adrenaline, and noradrenaline.....	21
Figure 1.9: Schema indicating the dopaminergic sources of midbrain and primary pathways of dopamine release	22
Figure 1.10: Steps of Krebs Cycle (Citric acid cycle)	25
Figure 1.11: Reaction of glucose and D-gluconolactone with chemical structures ...	26
Figure 2.1: The design shows the dimensions used in the production of the screen-printed electrode and its components.....	33
Figure 2.2: Fabrication steps of the MWCNT/SPE using screen printing.....	34
Figure 2.3: Flexible SPE (a), bent SPE (b), side view of the developed SPE connector (c) and front view of SPE connector and SPE (d).....	35
Figure 2.4: Modification steps of flexible glucose biosensor	36

Figure 2.5: Experimental setup for the 3 different samples (1=acetate paper, 2=MWCNT/SPE, 3=flexible glucose biosensor).....	38
Figure 3.1: CV curves of SPE electrodes fabricated with different amounts of MWCNT (a), $I_{p,a}$ and $I_{p,c}$ of an SPE in FcCH_2OH after every 10 cycles for a total of 100 cycles of bending test (b), CV curves from three different SPE electrodes (c), and one SPE over 15 days (d).....	40
Figure 3.2: Graph shows that curves at scan rates ranging from 5 to 2000 mVs^{-1} obtained by CV technique (a) and a graph showing the relationship between scan rate and $I_{p,a} - I_{p,c}$ (b).....	41
Figure 3.3: The EIS curve of the bare MWCNT-based and commercial SPE in 5 mM $\text{Fe}(\text{CN})_6^{-3/4}$ (a) and multiple CV curves of the SPE glucose biosensor in 1 mM FcCH_2OH (b)	42
Figure 3.4: SEM images of an electrode before bending (a and b) and after bending (c and d) at 100 μm and 200 nm	43
Figure 3.5: Chronoamperometric curves obtained in PBS containing dopamine in the range of 0 to 500 μM (a) together with a calibration curve (b) and selectivity results at 0.3 V (vs. Ag/AgCl) (c).....	45
Figure 3.6: Electrochemical mechanism in glucose detection using a redox mediator	46
Figure 3.7: DPV curves obtained in artificial sweat containing varying concentrations of glucose (a) together with a calibration curve (b) and glucose selectivity results at 0.3 V (vs. Ag/AgCl) (c).....	48
Figure 3.8: Cytotoxicity study of flexible MWCNT-based SPE. Fluorescent images of the dyed viable (green) and dead (red) cells for an acetate paper, flexible MWCNT-based dopamine sensor (bare electrode), flexible MWCNT-based glucose biosensor after 24 hour submersion (a), cell viability of L929 cells by MTT assay after 24 hour submersion (b).....	50

List of Tables

Table 3.1: Comparison of analytical performance of SPE-based dopamine sensors. 44

Table 3.2: Comparison of analytical performance of SPE-based glucose biosensors
..... 47

List of Abbreviations

WHO	World Health Organization
MWCNT	Multi-Walled Carbon Nanotube
SPE	Screen-Printed Electrode
DA	Dopamine
CNC	Computer Numerical Control
LOD	Limit of Detection
SEM	Scanning Electron Microscope
TUBITAK	The Scientific and Technological Research Council of Turkey
GNP	Graphene Nanoplatelets
TPU	Thermoplastic Polyurethane
PET	Polyethylene Terephthalate
PEDOT:PSS	Poly(3,4-ethylenedioxythiophene) Polystyrene Sulfonate
PCL/CHS	poly(ϵ -caprolactone)/chitosan
CV	Cyclic Voltammetry
PDMS	Polydimethylsiloxane
R2R	Roll-to-Roll
AgNW	Silver-Nanowire
CNT	Carbon Nanotube
SPCE	Screen-Printed Carbon Electrode
4-APBA	4-aminophenylboronic acid
GOx	Glucose Oxidase
HPLC	High-Performance Liquid Chromatography

LOQ	Limit of Quantification
GCE	Glassy Carbon Electrode
EIS	Electrochemical Impedance Spectroscopy
SWCNT	Single-Walled Carbon Nanotube
R _{ct}	Charge Transfer Resistance
MWCNT-COOH	Carboxyl Modified Multi-Walled Carbon Nanotube
PMMA	Poly(methyl-methacrylate)
f-MWCNT	Functionalized Multi-Walled Carbon Nanotube
PAMAM	Poly(amido mine)
d-MWCNT	Dendrimer Functionalized Multi-Walled Carbon Nanotube
HAP	Hydroxyapatite
Pd-Ni@f-MWCNT	Palladium-Nickel Nanoparticles decorated on Functionalized-Multi-Walled Carbon Nanotube
XRD	X-ray Diffraction
WE	Working Electrode
SWV	Square Wave Voltammetry
CVD	Chemical Vapor Deposition
NaOH	Sodium Hydroxide
YAG	Ytrium Aluminum Oxide Garnet
XPS	X-ray Photoelectron Spectroscopy
rGO	Reduced Graphene Oxide
NH ₂ -MWCNT	Amine-Functionalized Multi-Walled Carbon Nanotube
PANI	Polyaniline
Anti-TB	Anti-Tuberculosis
ETB	Ethambutol
TEM	Transmission Electron Microscopy
EDTA	Ethylene Diamine Tetraacetic Acid
CeBiVO ₄	Cerium-doped Bismuth Vanadate Nanorods

4-CY	4-Cyanophenol		
DPV	Differential Pulse Voltammetry		
Mn ₃ Co ₃ O ₄	Manganese Cobaltite		
FZD	Furazolidone		
EDX	Energy Dispersive X-Ray		
PVC	Polyvinyl Chloride		
EDC	1-Ethyl-3-(3-Dimethylaminopropyl) Carbodiimide		
AFM	Atomic Force Microscopy		
PTCA	Perylene-Tetracarboxylic Acid		
H ₂ O ₂	Hydrogen Peroxide		
L-DOPA	3,4-Dihydroxy-L-Phenylalanine		
ADHD	Attention-Deficit Hyperactivity Disorder		
ELISA	Enzyme-Linked Immunosorbent Assay		
EDS	Energy-Dispersive X-ray Spectroscopy		
CuNCs	Copper Nanocubes		
FLG	Few-Layer Graphene		
MLG	Multi-Layer Graphene		
Gr	Graphene		
Ac-CoA	Acetyl-CoA		
MODY	Maturity-Onset Diabetes of the Young		
SERS	Surface-Enhanced Raman Scattering		
GTP	Guanosine Triphosphate		
ATP	Adenosine Triphosphate		
EDC/NHS	1-Ethyl-3-(3-Dimethylaminopropyl) Hydroxysuccinimide	Carbodiimide/	N-
NEFA	Non-Esterified Fatty Acids		
4-MPBA	4-Mercaptophenyl Boronic Acid		

PEI	Polyethyleneimine
FAD	Flavin Adenine Dinucleotide
Fc-Nafion-GOx	Ferrocene Nafion-Glucose Oxidase
Ir-Zne	Crystalline iridium (III)-Zn (II) coordination polymers
CoTCIDPc	Tetracinamide cobalt (II) Phthalocyanine
β -CD	β -cyclodextrin
FcCH ₂ OH/FMA	Ferrocene Methanol
PBS	Phosphate-Buffered Saline
NaCl	Sodium Chloride
NH ₄ Cl	Ammonium Chloride
AA	Ascorbic Acid
UA	Uric Acid
NaOH	Sodium Hydroxide
DMEM	Eagle's Minimal Essential Medium
ΔE_p	The Peak-to-Peak Potential Separation
DMSO	Dimethyl Sulfoxide
CE	Counter Electrode
FBS	Fetal Bovine Serum
RSD	Relative Standard Deviation
KCl	Potassium Chloride
FTO	Fluorine-doped Tin Oxide
MoS ₂	Molybdenum Disulfide
AuNS	Gold Nanospikes
PNR	Polyneutral Red
AuNP	Gold Nanoparticles
ERGNR	Electrochemically Reduced Graphene Nanoribbon
GO	Graphene Oxide

CHI	Chitosan
dPIn	Doped-Polyindole
Nf	Nafion
Py	Pyrrole
APBA	Aminophenylboronic Acid
DHB	2,5-Dihydroxybenzaldehyde
PB	Prussian Blue
PAA	Polyacrylic Acid
P3ABA	Poly(3-aminobenzoic acid)
Ti ₃ C ₂	Tyrosine Nano Layer
PolyDADMAC	Polydiallyldimethylammonium chloride
NAD	Nicotinamide Adenine Dinucleotide
MTT	3-(4,5-Dimethylthiazol-2-yl)-2,5-Diphenyltetrazolium Bromide

List of Symbols

Ω	Electrical resistance [ohm]
sqr	Area
mil	Length
$^{\circ}C$	Temperature
ε	Total strain
$\%$	Percentage
M	Molarity
L	Liter
$v^{1/2}$	Square root of the scan rate
R^2	The coefficient of determination
S/m	Conductivity [Simenes per meter]
Fc	Ferrocene
A	Electric current
Sp^2	One of a set of hybrid orbitals
Π	Pi bonds
σ	Sigma bonds
Rct	Charge transfer resistance
Li	Lithium
Cu	Copper
Fe	Ferrum (Iron)
Co	Cobalt
Ni	Nickel

<i>Ar</i>	Argon
<i>V</i>	Volt
<i>Torr</i>	Pressure
<i>mg</i>	Weight
<i>m²/g</i>	Specific surface area
<i>mV/s</i>	Scan rate
<i>Ag/AgCl</i>	Silver/Silver Chloride
<i>cm²</i>	Area
<i>ΔE_p</i>	Potential between two peaks
<i>U/ml</i>	Activity of enzyme is quoted in units per ml
<i>aq</i>	Aqueous
<i>I_{p,c}</i>	Current of cathodic peak
<i>I_{p,a}</i>	Current of anodic peak

Chapter 1

Introduction

1.1 Screen Printing

The screen printing technique involves passing a thixotropic liquid through a mesh screen to create a specific image on a substrate. Shear thinning of thixotropic liquid is time-dependent and improving this property ensures homogeneous dispersion of the formed films [2]. As seen in the Figure 1.1, the overall screen printing system has components such as squeegee, stencil frame, paste/ink and substrate. The squeegee is moved across the screen to fill the mesh openings with thixotropic liquid, causing the screen to momentarily touch the substrate along a line of contact. The liquid then passes onto the substrate and when the squeegee is lifted off the screen, the screen is disconnected from the substrate. A single color is printed with each screen, so several screens must be used to produce a multicolored image or design [3].

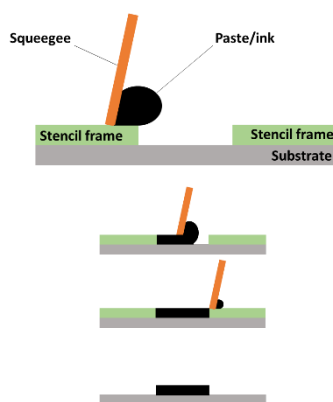


Figure 1.1: Schematic of the screen-printing system

There are many production parameters that improve the efficiency of the screen-printing method, these parameters can be listed as viscosity, ink geometry, repeating printing time, screen counting mesh, sintering temperature and time. Total number of wires per linear inch is called number of mesh. The number of times an ink/paste printing is applied is determined by repeating time. Furthermore, quality of the printed ink/paste is important, and is related to the rheological properties of the ink/paste. For quality ink/paste depends on parameters such as amount of solvent, binder and solid loading optimizing these factors also plays a role in improving the stability, electrical, electrochemical, mechanical and physical characteristics of printed electrodes. Ink preparation is concluded with a dispersant, a solvent, a binder and composite powder. Binders improve the connection of the particles in ink/paste, and content of binder is effective on ink/paste rheology. Besides such parameters, the improvement of quality of ink/paste is depends on thickness of the printed layer, and mixing process. In addition, a high binder content causes binder combustion after sintering and increased porosity, thus producing low-density thick films [2]. For this reason, the development of room temperature curable inks/pastes that do not require sintering has gained momentum in recent years. Such technologies have wide applications in the production of wearable electronics such as wearable sensors and smart clothing [4]. In a study on the development of low temperature curable conductive ink, a skin-compatible graphene-based ink was developed. The ink was obtained by mixing graphene nanoplatelets (GNP), which are abundant, mechanically strong, chemically inert, and highly conductive, and thermoplastic polyurethane (TPU) binder in a certain mass ratio. Followed by that, ink was printed on the polyethylene terephthalate (PET) surface with screen printing method and was cured for 15 min at 120 °C. Inkjet printing requires low-concentration inks, which limits the conductivity of printed tracks. Screen printing technique was preferred in this study because of its advantages such as simple, scalable, flexible, and fast. Also, rheological analysis of the ink was done. Then, electrochemical, morphological, and mechanical characterizations were made. As a result, stretchable conductors that remain conductive even under 100 % strain are realized by screen printing. The layer resistances of these conductors were measured as $34 \Omega \text{ sq}^{-1} \text{ mil}^{-1}$ after drying at 120 °C [5]. Wearable electronics can be developed for functions such as health monitoring systems, communication, and warming the body. In this sense, smart jackets containing flexible screen-printed heaters are a

popular wearable technology that can maintain body temperature and provide temperature feedback of the environment [6]. In recent years, the use of flexible printed heaters has increased frequently in targeted drug release, in the construction of smart and soft devices, and in areas such as thermotherapy. In this study, MWCNT and a polymer (poly(3,4-ethylenedioxythiophene) polystyrene sulfonate) based ink was evolved and printed on flexible surface, and also electrode was cured at room temperature. Consequently, layer resistance of this fabricated structure was obtained as $51.31 \pm 0.25 \Omega/\text{sqr}$ [7].

1.1.1 Screen-Printed Electrodes (SPE)

Screen printing is a technique of producing paintings with stencils, rooted in ancient Chinese art. It is based on applying a pre-designed stencil to various surfaces by pressing an ink from a mesh screen. Screen printing has a wide variety of uses such as clothing, artwork, posters, aeronautics, automotive, electronic circuits and sensor technologies [8]. It is especially used in modern times for mass production of electronic circuits and to meet the increasing demand for miniaturization in the global world. Screen printing technology has replaced ordinary wires to carry current without excessive voltage drop [9]. Innovative printing technologies facilitate the development of simple, disposable, cost effective and portable flexible devices like implantable biomedical devices and wearable biosensors. Screen printed electrodes (SPE) appear as innovative printing technologies in the field of sensors, and they present disposable, low-cost, flexible depending on the substrate used and portable electrochemical sensors. This technology is produced basically by printing conductive ink on mesh screens for creating the reference, counter and working electrodes on a substrate (polietilen tereftalat (PET), polyimide, plastic, ceramic). Preparation of conductive inks generally are composed of a mixture of a conductive material (such as metal, carbonaceous materials), a binder (resins, polymers) and additives [10]. Then, the prepared conductive ink is printed on the flexible substrate and the electrodes are covered with insulating material to identify the electrode measurement area and contact points [11]. SPEs are used in many different areas such as environmental, food, pharmaceutical, clinical laboratories and point of care. Topsoy et al. modified a commercial SPE with poly(ϵ -caprolactone)/chitosan (PCL/CHS) nanofibers prepared via electrospinning technique for detection of diazinon which is known as non-

systemic organophosphate pesticide. Electrochemical measurements of the produced SPE were made using cyclic voltammetry (CV) and the detection limit was 2.888 nM, obtained over a linear concentration range (3 nM–100 nM). In that study, diazinon repeatability, storage and selectivity of the developed sensor was also studied. Furthermore, recovery values determination of diazinon found as 93.27–108.30 % in the tomato juice sample. The developed PCL/CHS nanofiber-modified MWCNT-SPE's high sensitivity, high selectivity and low interferences had been put forth for the detection of pesticide [12]. Printing SPEs on solid substrates such as ceramics, as well as flexible substrates such as PET and polyimide, is just as common. The use of flexible substrates has a great importance in the development of wearable biosensor technologies. In this context, in the study of Zoerner et al., ammonium ion measurement was carried out in human sweat with an electrode produced by screen printing method with the help of a portable device. The produced carbon SPE was tested in real human sweat and as a result the detection limit was obtained as 0.3 mM [13]. In another study conducted by Mazzaracchio et al., an SPE electrode was developed on a polyimide substrate for pH measurement. A graphite-based ink for the working and counter electrodes and a silver ink for the reference electrodes were used in the construction of the SPE. The developed electrode was combined with a flexible integrated circuit board for pH measurement in sweat and wireless transmission of data was performed. The developed sensor was tested in vitro, demonstrating a comparable accuracy in other pH sensors, with the advantages cost-effectiveness, requiring few μL of sweat sample, miniaturized, and real-time data [14]. In wearable technologies, the sensing component is as important as the substrate. The sensing component must meet requirements such as stability, reproducibility, response time, lifetime, selectivity, accuracy and reliability. In particular, flexibility is an indispensable feature of wearable sensor technologies [15]. In this context, screen printing inks have been produced from various materials. In a study conducted by Huttunen et al., stretchable silver wires in various shapes on a flexible polydimethylsiloxane (PDMS) substrate were developed by roll-to-roll (R2R) rotary screen-printing method for wearable technologies. Printed silver wires with different geometries were characterized by stretching tests. As a result of the test conducted by applying repeated 20 % strain over 100 cycles, silver wires showed sufficient conductivity for signal transmission. Silver wires developed in this study for wearable technology can be applied for strain sensors,

sensor electrodes and signal transmission [16]. In another study where a water-based ink was developed, stretchable conductors and wearable thin-film transistors were produced on flexible PET from silver-nanowire (AgNW) ink. Developed ink had a low thermal annealing temperature of 150 °C, and with high conductivity as $4.67 \times 10^4 \text{ S cm}^{-1}$ [17]. Kim et. al. developed a wristwatch-type wearable Na^+ sensor device. Ultrathin screen-printed sensor with high electrical conductivity of $1.49 \times 10^4 \text{ S m}^{-1}$ and good mechanical flexibility was fabricated by graphene ink. Sodium ion sensor showed an excellent electrochemical sensing performance when it was bent. Moreover, real-time detection sweat sodium ion detection was shown [18].

1.1.2 Screen-Printed Carbon Electrodes (SPCE)

Carbon is a versatile element that can be found in various morphologies such as graphite, graphene, diamond (cubic), Q-carbon (amorphous), and carbon nanotubes (CNTs). Those carbon materials are used broadly for the fabrication of biosensors because of existence in nature, low cost, the low background current, taking part in surface modification, and easy fabrication. In addition to their electrochemical activities, good conductivity and physical durability, carbon nanomaterials have a high surface area to bind biomolecules (enzymes, antigens, antibodies, etc.) to the electrode surface [19]. By incorporating the advantages of carbon materials into the disposable, low-cost, miniaturization properties of SPEs, high-sensitivity, biocompatible, and specific screen-printed carbon electrodes facilitate the biosensor fabrication. SPCEs are extensively employed in industrial applications and especially in point-of-care. Consisting of a carbon material and a binder, SPCEs have a simple production method. Furthermore, they can be applied to mass production, and commercial ones are used in cholesterol, glucose, urea, uric acid, lactate, creatinine and hemoglobin sensing [20]. The measurement of amino acids is at least as important as these biomolecules. In order to detect some amino acids, Naqvi et al. developed a SPCE with carbon black. Developed electrode was modified with iron, and used in detection of serine, valine and phenylalanine. As a result, linear responses ($R^2 = 0.99836$ for serine, 0.99889 for valine, and 0.99551 for phenylalanine) were obtain from iron modified SPCE [21]. SPE's can be produced by printing on paper as well as surfaces such as ceramic, PET, polyimide, and plastic. Regarding this, in a study conducted by Rungsawagand et al., SPCE was produced on filter paper and the produced electrode coated with 4-

aminophenylboronic acid (4-APBA) was used for glucose detection. In this study, a graphite-based ink was obtained, and the triple electrode system was printed on Whatman filter paper. Chronoamperometric measurements were taken to observe the electrochemical measurement ability in real samples (tea, energy drinks, juice, soft drink, and blood serum). In light of measurements, it was found that the proposed electrode had a high sensitivity, wide linearity, high stability with 3 min response time [22]. Many efforts have been given for development of SPCE. Screen printing inks prepared from carbon nanomaterials produced with different techniques play an important role in improving SPCEs. Carbon nanotubes (CNTs) are the most popular of the carbon nanomaterials. CNT-based SPCEs can be preferred due to their excellent properties such as low detection limits, great sensitivity, fast electron transport, and selectivity [23, 24]. With regards to these nanomaterials, in a study multiwalled CNT-based SPCE was developed for sensitive glucose detection. MWCNT was manufactured by catalytic chemical vapor deposition method, and MWCNT-based ink was produced for printing SPCE. Then, fabricated SPCE was modified glucose oxidase (GOx) enzyme. Glucose concentrations were measured electrochemically, and limit of quantification (LOQ) was obtained as 0.14 mM. Additionally, lifetime of electrodes were two weeks [25]. More sensitive measurement of biomolecules can be achieved by modifying SPCEs with nanoparticles. In this context, manganese modified disposable SPCE was fabricated for chloride ion detection in sweat. In consequence, the sensor indicated detection range from 5 mM up to 200 mM with a good selectivity, and a good sensitivity of $3010 \pm 60 \mu\text{A} (\log \text{mM})^{-1} \text{cm}^{-2}$. Thus, SPCE was developed for cystic fibrosis with the LOD as $17 \pm 6 \mu\text{M}$ [26].

1.2 Carbon Nanomaterials

Nanotechnology has offered new perspectives in materials science and engineering in this field. In particular, it is clear that carbon nanomaterials are a technology that allows the creation of energy storage and conversion devices. In this regard, carbon nanomaterials demonstrate better performance than other conventional energy materials with their electrical, mechanical, morphological and optical features. Carbon nanotechnology materials such as graphene, fullerenes, and CNTs are promising for the production of electrochemical sensors [27]. Such materials are highly preferred in development of electrochemical biosensors and sensors by means of their fast electron

transfer, high durability, larger surface area, less overpotential, fine electrical conductivity, excellent sensitivity, good selectivity with excellent biocompatibility [28, 29].

The electron transfer and the electrochemical energy storage of redox mediators at CNT-based electrochemical sensors were also widely reported [30]. Synergistic application of superior properties of redox mediator with the many advantages of CNTs leads to the production of ideal electrochemical sensors. Redox mediators can lower the overpotential, and in their oxidized and reduced states, it can serve adequate chemical stability. Furthermore, redox mediators react rapidly with the enzyme in enzyme sensors, helping rapid electron transfer between the enzyme and the electrode [31]. Examples of redox mediators are quinones, Prussian Blue, methyl viologen, ferrocene and derivatives [32]. Among them, methyl viologen are extremely toxic, but ferrocene derivatives have low toxicity, in this way making them very biocompatible to manufacture wearable electrodes. Ferrocene and derivatives as redox mediators are significant and all-purpose in glucose biosensors field. Ferrocene mediators are known for their insensitivity to O₂, high physicochemical stability, steadiness in their oxidation/ reduction state, and excellent catalytic properties at low redox potentials. Furthermore, ferrocene and its derivatives are comparatively stable in air. Also, in enzyme biosensors, the redox mediator reverts after it is oxidized by the enzymes during the measurements [33]. In addition to these features, ferrocene derivatives are utilized as mediators to measure epinephrine, glucose, hydrazine, dopamine and p-synephrine [34]. In this context, one study by Gutierrez et al. manufactured an electrode for selective glucose detection using a glassy carbon electrode that was deposited with MWCNT. MWCNT and GOx was mixed, and deposited on GCE by dropping. Cyclic voltammetry, electrochemical impedance spectroscopy and chronoamperometry techniques were made for electrochemical characterizations. Glucose monitoring were performed inside 5.0×10^{-4} M FcCH₂OH solutions that contain various glucose concentrations. As a result of the study, glucose monitoring showed a detection limit as 20 μ M and sensitivity was obtained as $3.2 \pm 0.2 \times 10^2$ μ A M⁻¹. Also, stability of the excellent biocatalytic activity was obtained by taking 30 th days (25 °C and 4 °C) and 3 rd months measurement of the electrode [35].

1.2.1 Multi-Walled Carbon Nanotubes (MWCNT)

Carbon nanomaterials exist in a wide variety of forms, and one of the nanomaterials is called carbon nanotubes (CNTs) are tubes formed by bonding sp^2 -hybridized carbon atoms in the form of a hollow cylinder of one-dimensional graphite. Single-walled carbon nanotubes formed by rolling a single graphite layer and multi-walled carbon nanotubes formed by rolling multiple nested graphite layers (at 0.42 nm intervals) can be classified as two different carbon nanotubes. Typically, while SWCNTs have diameter as 0.75–3 nm and length as 1-50 μm , MWCNTs have diameter as 2-30 nm [36]. Besides their nanosize, CNTs also have properties such as extremely high surface area, ultra-light weight, rich surface chemistry and electrostatic potential [37]. Both nanostructures have advantages for the applied sciences, but MWCNT has considerable advantages like thermochemical stability, cheap production cost, higher yield, and sustain its electrical properties. There are possible π - and σ - bonds that can be installed on the MWCNT structure (Figure 1.2). As well as these possible bonds that it can, MWCNT offers high strength, chemical inertness, extreme active surface area, and also small R_{ct} in aq and non-aq solutions. Those features of multi-walled CNT can be utilized in different fields as supercapacitors, conductors, field emitters, energy storage, thin-film coatings, electromagnetic shields and electrochemical electrodes [38].

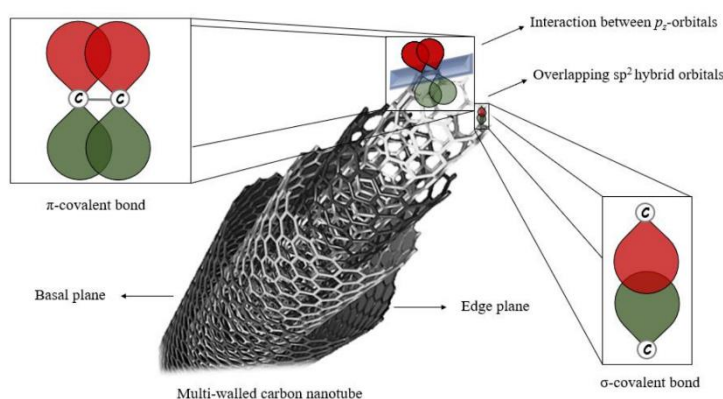


Figure 1.2: Structure of multi-walled carbon nanotubes, representing σ - and π -covalent bonds [38]

MWCNTs are frequently employed in electrochemical practices through low charge transfer resistance (R_{ct}), high detection sensitivity and electrocatalytic activity. When CNT is examined much more closely, it can be easily understood why it is used in analytical tools and electroanalytical research. In this line, it appears as a hexagonal lattice in which each of the carbons is bonded covalently with sp^2 orbitals to three other carbon atoms in the structure of CNT. Likewise, even number of electrons in the CNT structure makes it behave as a metal or semiconductor. Also, electron transfer of CNT is affected by tube diameter and chirality [38]. As presented in Figure 1.3, various SWCNTs (armchair, zigzag, chiral) are formed by rolling the single layer graphene from different directions. This state is called chirality and results in the SWCNT being either semiconductor or metallic. Armchair nanotubes have high conductivity. By turning round, a graphene layer at chiral direction of 30° , zigzag nanotubes are formed and they are semiconductors. In addition, MWCNTs are extremely electroconductive material that usually increased the current into the 10^9 A cm^{-2} levels. Also, MWCNTs have unique geometry, flexibility, stiffness, and superior Young modulus [39].

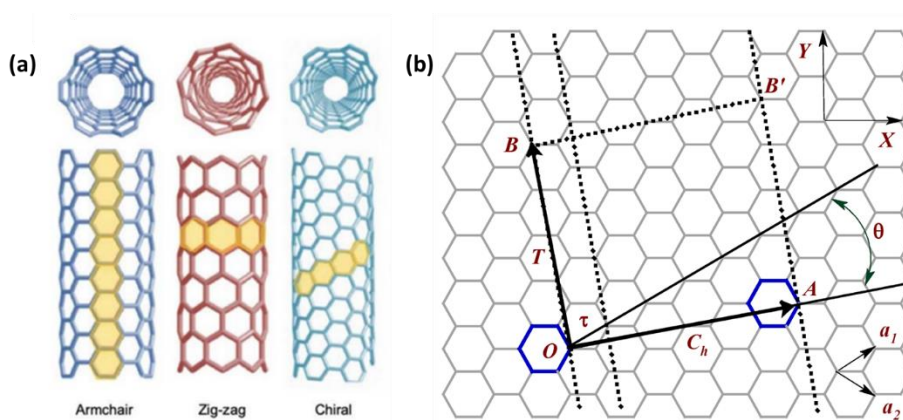


Figure 1.3: Types of the chirality of the SWCNTs (a), and honeycomb shape of graphene layer with the chirality (b) [38]

Discovered in 1991, carbon nanotubes are used in materials science, physics, chemistry and biosensor fields [40]. As mentioned above, MWCNT is used in many fields and many successful studies have been carried out on these issues. In one of these studies, Yu et al., high temperature resistant lithium batteries have been developed. Solid polymer electrolytes and carboxyl modified MWCNT (MWCNT-

COOH) were used in the construction of the battery to show good electrochemical behavior between 70 and 120 °C. Produced battery showed low polarization voltage for 1800 h at 70 °C [41]. Another study was conducted in the field of space technology. In space missions, it is very important to protect astronauts and spacecraft from radiation, and also that the materials used both provide radiation protection and are light in weight. In this line, in a study of Li et al., poly(methyl-methacrylate) /MWCNT (PMMA/MWCNT) nanocomposite was developed for radiation shielding. The MWCNT embedded in the PMMA matrix showed thermal stability compared to the pure polymer, and gave a good result in radiation shielding, although it did not show a significant effect in weight reduction [42]. The good mechanical properties of MWCNTs are used in various fields. In the field of ballistics, which is one of them, the contribution of MWCNTs to bulletproofing of various materials has been investigated. In the study, low and elevated speed effect tests were made using a gas gun assembly on Kevlar reinforced polymer matrix composites and MWCNT structure. As a result of the study, addition of functionalized MWCNT (f-MWCNT) to Kevlar matrix has increased the matrix toughening [43]. The biocompatibility of MWCNTs is as important as their mechanical properties. Its biocompatibility properties have been studied in many biomedical fields, from tissue engineering to biosensors. In a study, poly(amido mine) (PAMAM) dendrimer was covalently functionalized with MWCNT (d-MWCNT) and then a composite was formed with hydroxyapatite (HAP) and d-MWCNT to improve bioactive, drug release /loading, and mechanical properties of hydroxyapatite. According to composite characterization, composite was porous, hydrophilic, mechanically strong, protein adsorbing, and bioresorbable. The composite of d-MWCNT with HAP showed a 30-fold curcumin loading over HAP. It showed a delay of 1.7 fold in curcumin release. In addition, in vitro studies have been performed using MG-63 cells, and functionalized MWCNT-HAP composites have been shown to promote differentiation, proliferation, matrix mineralization and survival of osteoblasts. This MWCNT-based material is promising in the body drug delivery system in bone tissue engineering [44]. Finally, there are many successful studies in biosensor discipline. Karimi-Maleh et. al. decorated functionalized-multiwall carbon nanotube with palladium-nickel nanoparticles for non-enzymatic electrochemical glucose sensor. Different characterization methods were used (transmission electron microscopy (TEM), XPS,

raman spectroscopy and XRD). The glucose measurement was performed by CV technique, and as a result, detection limit was acquired as 0.026 μM and sensitivity was obtained as 71 $\mu\text{A mM}^{-1} \text{cm}^{-2}$ were obtained. Additionally, applicability for specimen analysis, stability, and reproducibility were shown. Designed sensor was compared with commercial glucometer, and obtained results demonstrated that MWCNT is promising for electrochemical glucose detection [45].

1.2.2 MWCNT Production Techniques

MWCNTs can be produced by laser ablation, chemical vapor deposition, electric-arc discharge etc [36]. One of the oldest known CNT production methods is electric arc discharge. The technique can be defined as evaporation of carbon with plasma by bringing it to high temperatures as a conventional and easy device. With this method, hollow graphite tubes are obtained with graphite powder and transition metals (Co, Ni or Fe). In Figure 1.4, an arc-discharge system for production of CNTs was given. Inert gas is given to vacuum chamber, and at the same time two carbon electrodes are roomed in this system. Then, the pressure in the system fixes, the system is powered. For the creation of the electric arc, positive electrode must be slowly brought closer to negative electrode. Thus, electrodes switch to plasma state. When the electric arc is stabilized, carbon nanotube is built up on negative electrode and rods are gradually removed. When the desired length is achieved, system is not powered, and system is allowed to cool. Furthermore, pressure of inert gas supplied to system is kept at 50–600 Torr and the other parameters are generally as follows: temperature as 2,000–3,000 $^{\circ}\text{C}$, current as 100 amps and voltage as 20 V. These parameters are essential for the production of efficient SWCNTs or MWCNTs. CNTs produced by this method are generally short in length and diameter is about 10 nm. The technique is comparatively simple and offers an efficiency of 30 % in production. In addition, the impurities of CNTs produced by this method are higher than other methods, but the consistency in the dimensions of the tubes is random [46]. In a study, Zhao et al. used MWCNTs by arc-discharge method for building up non-enzymatic glucose sensor. Copper nanoparticles were also used in the structure of the produced electrode. In non-enzymatic oxidation of glucose by 0.1 M sodium hydroxide, produced MWCNT-based electrode showed high electrocatalytic activity. Results of electrochemical measurements showed great linearity in the 0.5–7.5 mM concentration range with

sensitivity as $922 \mu\text{A mM}^{-1} \text{cm}^{-2}$ and also showed fast response with detection limit as $2.0 \mu\text{M}$. This study demonstrated that Cu-MWCNTs electrodes produced using arc discharge method are good candidates for reliable and non-enzymatic glucose determination [47].

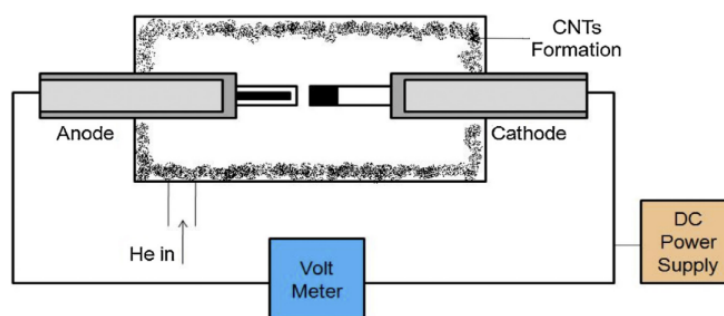


Figure 1.4: Schematic of arc discharge chamber for production of CNTs [46]

Laser ablation is a relatively new method of producing nanotubes. As in the electric arc discharge method, it is based on the logic of evaporating the carbon with high energy and depositing it on a substrate. Carbon is evaporated using a laser source in a noble gas environment under high temperature in a chamber as in Figure 1.5. The figure shows the complete system and as shown in the figure, a laser beam (usually a yttrium aluminium oxide garnet (YAG) or CO_2 laser) enters the system and is sent to the target inside the chamber. Carbon is evaporated at high temperature in the presence of noble gas and CNT is obtained. It was reported in another study that pure graphite should be used for MWCNT production. For the most efficient MWCNT production with this method, a temperature of $1200 \text{ }^\circ\text{C}$ should be used. The lower reaction temperature decreases the quality of CNTs produced [46].

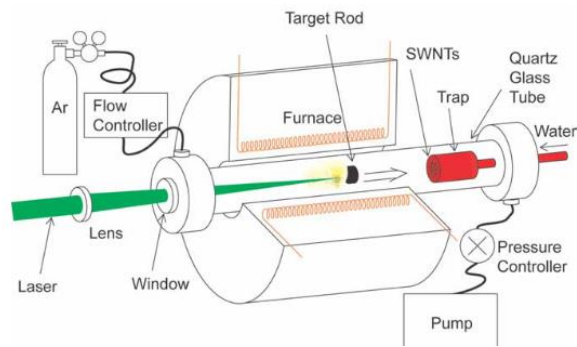


Figure 1.5: Schematic of laser ablation chamber for production of CNTs [48]

Lastly, one of the popular known CNT production methods is CVD. The process of casting a solid on a chemically, preheated metal is called CVD. Production of powders, coatings, fibers, thin or thick films and monolithic components are possible with CVD method. With this method, many non-metallic elements (silicon, carbon), most metals, numerous compounds including oxides, carbides, intermetallics and nitrides can be produced. The setup of the CVD method is given in Figure 1.6. The system contains a quartz tube of through two furnaces. There are two chambers in this system, at first Ar gas is supplied to the system to provide non-oxygen atmosphere, temperature of second chamber is increased to intended reaction heat. Then, flow of gas is turned off, temperature of first chamber becomes 150 °C. Afterwards, flow of gas turned on, and hydrogen and acetylene (C_2H_2) gas released free. The catalyst is placed in middle of first chamber. Growing CNT is carried out in the second furnace and collected there [46]. Temperature is an important parameter in CVD production and MWCNT is produced at low temperatures (600-900 °C), while SWCNT is produced at high temperatures (900-1200 °C). As can be seen from this, SWCNTs require higher energy to be produced, so MWCNTs are easier to produce than SWCNTs [48].

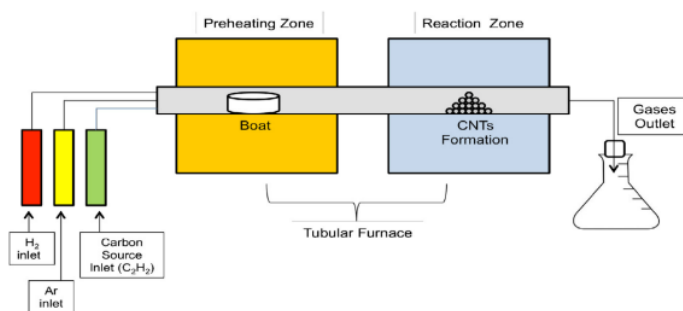


Figure 1.6: Schematic of chemical vapor deposition for production of CNTs [46]

Among the CNT production methods, CVD method has more beneficial than laser ablation and arc discharge. The reactor model and reaction operation of CVD method is basic, less complex than other methods. Excessive number of energy is essential for laser blasting and arc discharge. The energy required is neither useful nor economical for large-scale production. Also, such large graphite is difficult to use in large-scale production, thus limiting its use in large-scale processes. Moreover, both processes require purification of nanotubes from undesired forms of carbon or catalyst, and the designs used to accomplish this process are both difficult and expensive. In addition, the CVD method is more economical than other CNT production methods [46]. It has been widely used because of the many advantages of producing CNT by CVD method and there are many studies on this subject. To exemplify, in one study, for measurement catechol in wastewater, novel electrochemical platform was fabricated. MWCNT prepared by the CVD method was modified to the detection area of the electrode. Chronoamperometry measurement was implemented for enzymatic catechol detection (0.8 to 3.0 mg/L). Consequence, MWCNT based biosensor was showed LOD as 0.25 mg/L, and in addition to this the reproducibility acquired as less than 4.95 %. Also, lifetime of the sensor was worked out, and found as more than 30 days. This study showed that the MWCNT based catechol biosensors can alternating way in order to measure other phenolics in environmental specimens. [49].

1.2.3 MWCNT-Based SPCE Biosensors

Nowadays, great strides have been made in development of SPE-based electrodes. Besides the various advantages of SPE-based sensor systems, numerous materials which may be used in working electrode (WE) production highlights the versatility of these sensors. Owing to low background current, simple renewable surface, low cost, versatility, low background current and chemical stability features, carbon materials are frequently used in SPE structure [50]. Thanks to the versatility of SPCEs, WE may be deposited with carbon nanotubes for giving the electrochemical system unique features such as ideal electrical conductivity, rapid electron transfer, larger surface area, superior durability, less overpotential, high sensitivity, high selectivity and excellent biocompatibility. MWCNTs combined with their excellent features make SPCE biosensors indispensable devices for analytical purposes. Also, remarkable electrical conduction and excessive surface (approximately $1600 \text{ m}^2 \text{ g}^{-1}$) of the MWCNTs increases miniaturization and portability of the systems. These features are highly used in electrochemical sensors and nowadays, MWCNT-based electrochemical sensors are preferred in pharmacology, environmental analysis, sanitary surveillance, medicine, clinical diagnostics and forensic [38]. In this context, in one study, immensely sensitive glucose biosensor was developed with immobilizing GOx on SPCE. For increasing electrochemical sensing capacities and electron transfer, amine-functionalized MWCNT (NH_2 -MWCNT)/rGO hybrid complex was prepared. NH_2 -MWCNT provided forming H_2 bonds between carboxyl of GOx and amines of MWCNT. Immobilization of the GOx enzyme on the SPCE was provided by polyaniline (PANI) as a conducting polymer that can provide great electrochemical activity for glucose sensing. Electrochemical glucose analysis in human blood specimen had been made over modified SPCE by using chronoamperometry. Also, electrochemical analysis of bare SPCE and modified SPCE was conducted and compared. As a result, it was found that modified SPCE had enhanced reduction current 13.43 times when compared with bare SPCE. Also, the glucose biosensor showed wide linear range (1–10 mM), great stability, detection limit as $64 \text{ }\mu\text{M}$ and sensitivity as $246 \text{ }\mu\text{A cm}^{-2} \text{ mM}^{-1}$. Produced sensor has potency for an effective glucose sensor [51]. Like the electrochemical biosensor example given above there are not only electrochemical biosensors for diagnostic purposes, there have also been good studies in the field of pharmacology that can be considered a branch of medicine. In a study,

Nafion/MWCNT/SPCE was evolved to electrochemically detect ethambutol (ETB), that is one of the anti-tuberculosis drugs. ETB is an organic cation, and this feature can be used in electrochemical studies. In this study, electrochemical detection of ETB was wanted, and the anionic nafion polymer was used for easy detection of ETB. In this line, commercial SPE was prepared by modifying nafion and MWCNT on electrode surface. Then, produced electrode electrochemically characterized with EIS, and electrochemical measurements were made through CV and square wave voltammetry (SWV). Consequently, produced Nafion/MWCNT-SPCE presented a detection limit as 8.4×10^{-4} mg/ μ L with a good selectivity and sensitivity. Also, favorable reproducibility and repeatability were obtained. The produced electrode was promising for electrochemical ETB sensing [50]. In addition to the excellent properties of MWCNTs, the use of conductive polymers such as PANI ensures that the produced biosensors or electrodes have good electrical conductivity, are less affected by environmental conditions, and reduce costs. Furthermore, the π - π interaction between the PANI and MWCNT complex that can be formed, can increase sensor's sensitivity by rising the electron transfer rate. In a study, SPCEs were modified with EDTA, PANI together with MWCNT for electrochemical lead, mercury and copper ions detection. EDTA was used as a multidentate ligand in this study for formation of complexes by several heavy metal ions that help selective detection of metal ions. SWV was utilized electrochemical detection of aforementioned metal ions. Besides, the sensitivity, selectivity, reproducibility and stability studies of the non-polluting, low-cost, simple, and high-efficiency produced sensors were performed. Developed sensor demonstrated process simplicity and practicability with a limit of detection as 55.4 pM (copper), 22 pM (lead), and 17.8 pM (mercury). In the light of the data obtained, it is predicted that this electrode will help develop low-cost disposable electrodes that can provide simultaneous detection [52]. Another study was conducted in the field of environmental analysis. In that study, cerium-doped bismuth vanadate nanorods (CeBiVO_4) and functionalized-MWCNT (f-MWCNT) were modified on SPCE for sensing environmental hazardous compounds called 4-Cyanophenol (4-CY). The CeBiVO_4 was synthesized by hydrothermal method and characterized by optical and structural analysis. Electrochemical analysis was performed by DPV and CV methods. The f-MWCNT/ CeBiVO_4 SPCE presented excellent electrocatalytic properties for sensing of 4-CY with wide linear range of 0.001–1207 and 1307–3107

μM , and also LOD of 7.3 nM. Sensitivity of the prepared electrode was $0.05 \mu\text{A } \mu\text{M}^{-1} \text{ cm}^{-2}$ [53]. Sample collection and processing is an important parameter in biosensors. Many different body fluids can be collected and analyzed for many different target molecules. In spite of collecting blood samples is not that difficult a process, processing the blood sample is hard due to interferences (cells, immunoglobulins, proteins etc.). In those situations, sample dilution can be required to reduce the matrix effects and facilitate detection of target molecules [54]. Other biofluids (sweat, tear, saliva, urine etc.) have more basic composition than blood, but whole has different pH values. MWCNTs are chemically inertness [38], so they are resistant to the harsh conditions of biological fluids. Related to this issue, in a study, manganese cobaltite ($\text{Mn}_3\text{Co}_3\text{O}_4$)/MWCNT based SPCE sensor has been developed that can be used in the analysis of real samples. For this, at first $\text{Mn}_3\text{Co}_3\text{O}_4$ was prepared by a method called co-precipitation, and MWCNT / $\text{Mn}_3\text{Co}_3\text{O}_4$ complex was made by ultrasonication. Characteriation of this complex was performed via Raman, energy dispersive X-Ray (EDX), XPS, XRD, TEM, and FT-IR. Then, a SPCE was modified by $\text{Mn}_3\text{Co}_3\text{O}_4$ /MWCNT nanocomposite by drop-casting, and the prepared electrode was used for electrochemical detection of antibiotic furazolidone (FZD). CV, EIS, and DPV methods were used for its electrochemical analysis. As a result, the prepared electrode demonstrated excellent electroanalytical characteristics due to the synergistic effect of MWCNT and $\text{Mn}_3\text{Co}_3\text{O}_4$. Electrochemical analysis showed a broad linear range from 0.05 to 650 μM and a LOD as 0.55 nM for FZD sensing. Furthermore, reproducibility and good storage stability have been successfully demonstrated. As an important part of the study, the real-time application and the recovery of the produced electrode was studied by serum and urine samples [55]. In another study, Wang et al. developed SPCE with MWCNT ink. Ink was prepared by mixing MWCNT powder and 2 % (w/v) polyvinyl chloride (PVC). Prepared mix was printed on alumina ceramic plates using patterned stencil screens and cured for 1 h (at 150 °C), then allowed to cool to room temperature. For production of glucose biosensor, GOx and then 0.5 % nafion were modified on the WE of the prepared electrode. Remarkably, such thick-film CNT sensors are mechanically stable and exhibited high electrochemical reactivity [56]. The synergistic effect of SPCE and MWCNT has enabled the production of disposable sensors that are not affected by

chemical changes, can measure with high precision and offer a stable electrochemical response.

1.3 Enzyme Biosensors

When electrochemical biosensors are combined with enzymes, they form enzymatic electrochemical converters and are used in many fields because of their promising properties. In addition, enzyme biosensors can selectively detect the target molecule. The factors affecting this selectivity can be listed as the specificity of the enzyme, the type of biosensor (first, second or third generation), the complexity of the sample, the electrode type and the modification of the enzyme to electrode surface. For the enhancement of capabilities of enzyme biosensors, the choice of sensing surface, immobilization method, membranes and modifiers is important [57]. In particular, the immobilization method is of great importance. The stability of the enzyme on the electrode surface, the accessibility of the target molecule to the active site during measurement, and the reusability of the electrode vary according to the correct immobilization and immobilization method. These are enzyme immobilization methods that can be used to increase the stability and reproducibility of detection: crosslinking, covalent bonding, adsorption, entrapment and encapsulation (Figure 1.7). Crosslinking is a widely used method that improves the stability, but conformational changes in the structure due to the using reagents, so it can affect the enzyme activity. Covalent bonding is a simple method that allows reuse. However, chemical formation of bonding may cause loss of enzyme activity. Adsorption is a simple at the same time cheap method and also not required reagents. Nevertheless, it shows lower efficacy. Entrapment is a fast and cheap technique that provides stability of the enzyme, but it may prevent diffusion of target molecule on to the enzyme's active site. Lastly, long term stability of the enzyme on electrode surface may provided with encapsulation. Likewise, the choice of electrode material is important for promoting stability, enzyme activity and selectivity. Therefore, material must be stable and chemically inert [58].

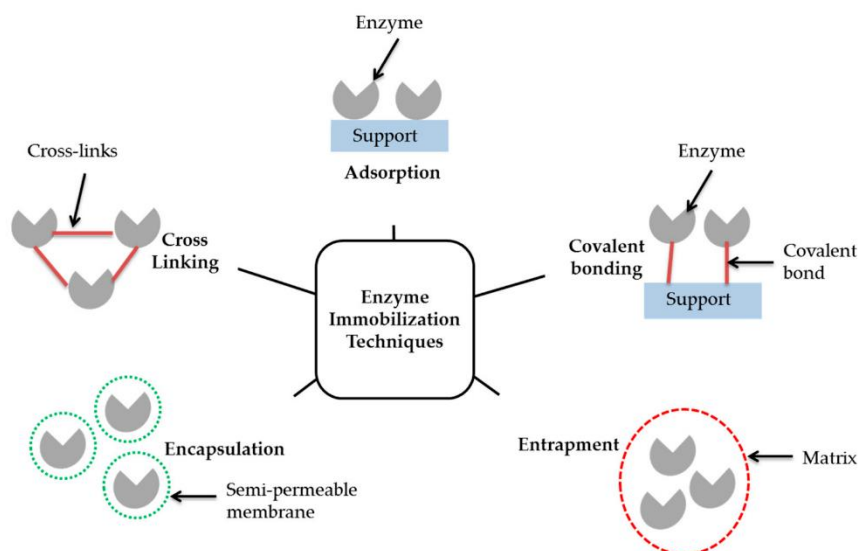


Figure 1.7: Schematic of enzyme immobilization techniques [59]

Lately, enzymatic biosensors have been evolved as wearable devices for non-invasive analysis of biomolecules (e.g., lactate, glucose, uric acid). Enzyme biosensors present selective and sensitive measurement with a low detection limit. The usage of SPEs in the making of enzyme sensors has become popular because SPEs are simple, disposable, small size, cost-effective and portable flexible devices. Also, SPEs allow film forming on the electrode surface [60]. The covering of the enzyme layer with a convenient permselective film can also help to prevent leakage of the enzyme from the electrode surface, to keep the electrode surface clean, and lastly, to make ready electrode for interacting with the species [61]. Akhtar et. al. fabricated electrochemical glucose biosensor with functionalized graphene. Au nanoparticles were sputtered for 180 seconds by using a sputter coater onto the SPE. Graphene oxide and 1-Ethyl-3-(3-dimethylaminopropyl) carbodiimide (EDC) were dropped onto the surface of the working electrode. 5 μL of glucose oxidase (GOx) (600 U/mL) was modified on the Au-SPE. The developed electrode was characterized by CV, and also AFM and SEM. Produced electrode indicated a limit of detection of 0.3194 mM and sensitivity as 3.1732 $\mu\text{AmM}^{-1}\text{cm}^{-2}$ for detection of glucose. This study highlights the potential of graphene [62]. In another study, SPE was modified with MWCNT for a selective and sensitive glucose detection. For this MWCNT was mixed and bound with perylene-tetracarboxylic acid (PTCA) through π - π stacking. Nafion was added to the prepared mixture and surface of SPE was deposited with mixture. Then, GOx was immobilized

on the SPE, aided with 1-Ethyl-3-(3-dimethylaminopropyl) carbodiimide/ N-Hydroxysuccinimide (EDC/NHS) chemistry, and GOx was dried for 1 hour at room temperature. Electrochemical measurements were performed by cyclic voltammetry, and as a result, sensitivity was found as $0.58 \mu\text{AmM}^{-1}\text{cm}^{-2}$ with detection limit of $35 \mu\text{M}$ in a linear range of 1–19 mM. In the study, MWCNT offered a high surface area for the adhesion of more enzyme molecules to the surface. It also increased the electrocatalytic activity, enabling the enzyme glucose sensor to measure more sensitively and selectively. Furthermore, the fabricated electrode was utilized for glucose measurement in blood serum. Therefore, enzyme sensors can provide a reliable measurement for sensitive and selective detection of some biomolecules [63].

Enzyme glucose biosensors can be divided into three classes depending on the electrochemical relationship between the enzyme and the electrode. The first of these is the first generation biosensors. They allow catalyzing glucose for generation of hydrogen peroxide (H_2O_2) that is oxidized at the surface of electrodes at a reasonably high redox potential. Furthermore, oxygen amount is a limiting factor for this type of biosensor, so a different and more advanced biosensor is needed [64]. Second generation uses a non-physiological electron acceptor for solving the lack of oxygen problem. These biosensors have a mediator (as electron acceptor) that is able to carry the electrons from enzyme redox center to the electrode surface. Mediators work as artificial electron transfer agents that facilitate electron transfer. The rapid transfer of electrons helps to prevent the oxidation of interfering species by lowering the operational potential of the biosensor. Mediators that are frequently used in this type of biosensors can be listed as transition metal complexes, quinone compounds, phenothiazine, ferricyanide and ferrocene derivatives [65]. Third generation biosensors do not have a mediator, and they can transfer the electrons from glucose to the electrode surface through the active site of the enzyme, also they work with a low operating potential. These sensors are inexpensive and more resistant to environmental conditions, close to the redox potential of the enzyme itself [64, 66]. The use of nanomaterials in the electrode structure is important for the production of third generation electrodes due to their properties such as increased electroactive area and roughness factor. Nanomaterials used in the construction of third generation biosensors include graphene, metal nanoparticles and carbon nanotubes. With their

high surface/volume ratios, they provide better communication between the electrode and the enzyme [64].

1.4 Dopamine

1.4.1 Importance of Dopamine

Dopamine (DA) is a neurotransmitter that plays a role in reward-guided learning and motivation [67]. It has substantial contributions to conduct impulses, regulate cognitive, endocrine, emotional, cardiovascular, renal, gastrointestinal and motor functions [68, 69]. At cellular level, 3,4-dihydroxy-L-phenylalanine (L-DOPA) is created by the hydroxylation of tyrosine. Then, dopamine is created by the decarboxylation of L-DOPA. In a study, it was demonstrated that DA is not only an intermediate in the production of certain hormones (epinephrine/adrenaline and norepinephrine/noradrenaline), but also a true neurotransmitter. In the Figure 1.8, synthesis of dopamine, serotonin, adrenaline, and noradrenaline are shown. The dopaminergic neurons of the human brain are located in the substantia nigra, ventral tegmental, and midbrain (Figure 1.9). DA behaves on specific receptors. Also, DA appears at several time intervals to help regulating activities of the organism for surviving. Dopamine can be detected in urine [70].

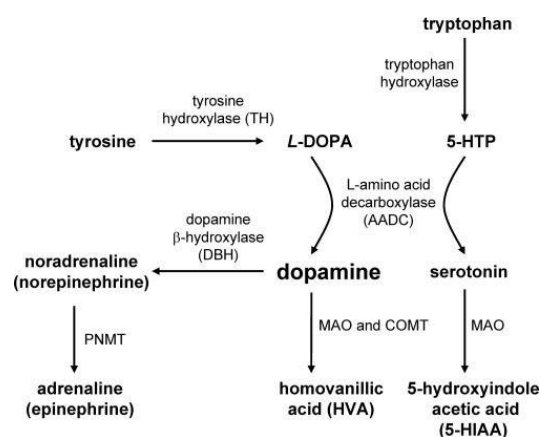


Figure 1.8: Pathways for synthesis of dopamine, serotonin, adrenaline, and noradrenaline [70]

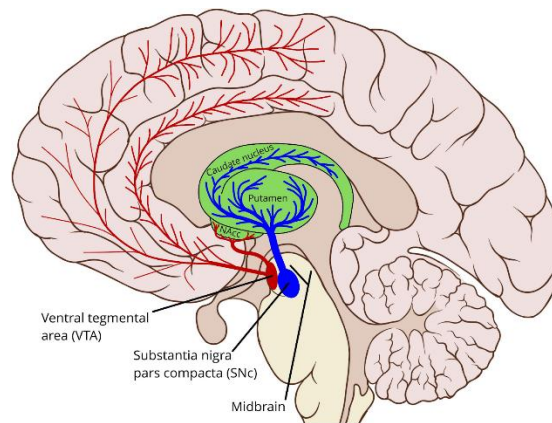


Figure 1.9: Schema indicating the dopaminergic sources of midbrain and primary pathways of dopamine release [71].

In normal conditions and in healthy person, the DA concentration in urine 52–480 ng/mL (0.3–3.13 μ M) [72], 15–30 pg/ml (97.9-195 μ M) in blood plasma [73], 0.01–1 μ M in extracellular fluid of caudate nucleus [74], and is around 18.9 pg/mL in saliva [75]. It is a well-known fact that some biomarkers are found in lower concentrations in sweat than in blood plasma. However, there are no studies on the perception of dopamine in sweat. In addition, the correlation between concentrations of L-DOPA, the precursor of dopamine, provides an estimate of dopamine levels in plasma and sweat samples [76]. Also, the level of levodopa in sweat is in the micromolar range. Therefore, with current technologies, the detection of dopamine in sweat can be reliably done via L-DOPA [77]. The abnormal levels of DA bring about major neurodegenerative diseases such as attention-deficit hyperactivity disorder (ADHD), Alzheimer's, Parkinson's diseases, Huntington's diseases, paragangliomas, and schizophrenia [75]. These diseases can affect the nervous system and threaten the patient's life, so it is important to monitor dopamine levels.

1.4.2 Dopamine Detection

Dopamine, which causes many neurological diseases, can be detected by conventional methods such as the electrochemical, enzyme-linked immunosorbent assay (ELISA), mass spectroscopies, high-performance liquid chromatography (HPLC), coulometry or fluorometry. On the other hand, these methods are complex, expensive and time-consuming [78]. But the electrochemical method is the proper method of detection of

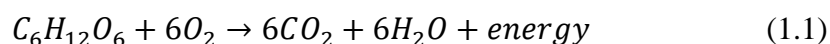
DA. Although species that coexist in real biological specimens have similar redox potentials with dopamine, many new materials and electrodes have been developed over the years to address this problem [79]. In this context, Ahmad et. al. prepared WO_3 rods by sol-gel method. The prepared material was characterized by SEM, energy-dispersive X-ray spectroscopy (EDS), XPS, and powder X-ray diffraction (XRD). Then, the WO_3 was dropped on SPE, and electrochemical analysis of the WO_3/SPE was performed for DA determination. Electrochemical measurements were made by square wave voltammetry (SWV) method. The WO_3/SPE presented good sensitivity as $3.66 \mu\text{A}/\mu\text{M cm}^2$ with a detection limit of $0.87 \mu\text{M}$. Furthermore, produced electrode indicated excellent selectivity with cyclic stability [80]. Dopamine exists in higher concentration in biological fluids like blood with uric acid. Electroactivity of uric acid and dopamine in terms of potentials very close to each other. So, selective detection of dopamine is very important. Dopamine exists in higher concentration in biological fluids like sweat with uric acid. Electroactivity of uric acid and dopamine in terms of potentials very close to each other. So, selective detection of dopamine is very important. For this, different techniques can be applied. One of them is the oldest method that is based on developing negatively charged electrode materials that repel negatively charged molecules and attract positively charged dopamine. In a study, a negatively charged material that bentonite clay was used for selective and successful detection of dopamine. Also, it was aimed to measure dopamine in the presence of ascorbic acid and uric acid by using pristine MWCNT in the fabrication of the electrode. SEM, EDX and XRD characterization methods were used for pristine MWCNTs and bentonite clay. Electrochemical analysis of dopamine was performed through DPV measurements at a scan rate of 20 mV/s . A linear response from 0 to $14 \mu\text{M}$ was obtained and the detection limit was 6 nM . Moreover, as a result of the electrochemical characterization, it was understood that produced sensor has a broad working surface with effective electron transfer properties. Effect of various parameters on efficiency of the electrode was studied, and optimal pH was discovered as pH 7.4, and the optimum accumulation time was found to be 40 s . The selectivity test was studied at the same concentrations as the amounts of ascorbic acid and uric acid in the blood. This study concluded that the produced electrode has good selectivity, and good long-term stability towards dopamine detection [81]. In another study, a selective and sensitive electrochemical sensor was developed for the dopamine

determination by fabricating copper nanocubes (CuNCs) and modifying them on to the few-layer (FGL) and multi-layer graphene (MLG). CuNCs were electrodeposited on graphene modified SPE. The produced nanomaterial was increased the sensing area of electrode and also, it characterized by various microphysical characterization methods. EIS, CV and DPV were used for the electrochemical analysis of the electrode, and the DPV method was used to monitor the oxidation of dopamine. As a result of the study, dopamine detection was obtained in the linear range of 0.001 – 100 μM . Moreover, the sensitivity was obtained as 196 $\text{mA}/\text{molL}^{-1}$ and the limit of detection was 0.33 nM. CuNCs-Gr/SPCE indicated good selectivity for dopamin detection in presence of other neurotransmitters [82].

1.5 Glucose

1.5.1 Glucose Metabolism

Glucose is one of the biological compounds that is most critical for life. Glucose, a potential energy source used for from glycolysis to growth, is formed as a result of the calvin cycle (photosynthesis) [83], and it is broken down into energy in cells with the help of glycolysis in the presence of oxygen (aerobic respiration). The basic formula for aerobic respiration:



Briefly, in the first stage of the respiration, glucose is converted into pyruvic acid. Then, in the presence of oxygen, it is used to extract more energy. 60 % of this released energy is used as heat energy in the body. This helps to protect body temperature for warm-blooded animals. Remaining energy can be used for growth, repair, muscular movement, maintenance of heartbeat and breathing of the organisms [84]. All this is achieved by glycolysis followed by the Krebs cycle (Citric acid cycle) (Figure 1.10).

The pyruvate, that is formed after glycolysis, oxidizes to form acetyl-CoA (Ac-CoA), and Ac-CoA is converted to citrate with the help of citrate synthase and enters the Krebs cycle. Pyruvate can also enter the Krebs cycle to form oxaloacetate via a reaction catalyzed by pyruvate carboxylase. Citrate formation is followed by seven sequential reactions to regenerate oxaloacetate, and also two CO_2 molecules are released during

the Krebs cycle. After producing citrate, the citrate is isomerized by a dehydration-hydration sequence to yield (2R,3S)-isocitrate. Further, alpha-ketoglutarate and a CO₂ molecule come out as result of the enzymatic reaction between isocitrate and isocitrate dehydrogenase. Another enzymatic decarboxylation and oxidation reaction causes to form succinyl-CoA from alpha-ketoglutarate. The hydrolysis of succinyl-CoA to succinate occurs. Dehydrogenation of succinate to fumarate causes to form flavin adenine dinucleotide (FAD). Fumarate catalyzed by fumarase is transformed to malate by using water molecule. The last step of the Krebs cycle is fulfilled with nicotinamide adenine dinucleotide (NAD)-coupled oxidation of malate to oxaloacetate is catalyzed by malate dehydrogenase. In one complete cycle, the energy is trapped by the production of three molecules of NADH, one molecule FADH₂ and one molecule of nucleoside triphosphate (GTP or ATP). This series of events occurs in the matrix of mitochondria in eukaryotes, while in prokaryotes it takes place in the cytosol [85].

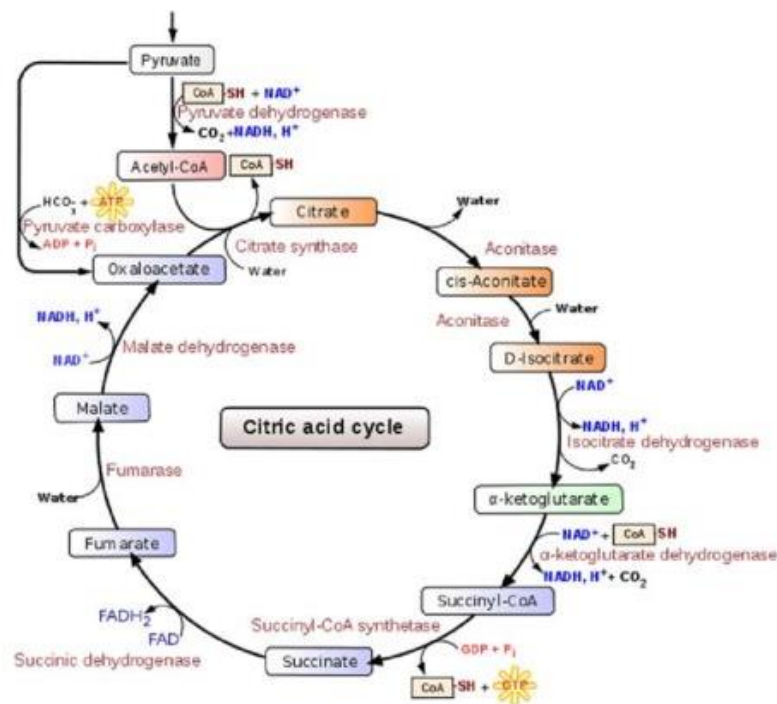


Figure 1.10: Steps of Krebs Cycle (Citric acid cycle) [85]

In the most common glucose biosensor systems using GOx, it can oxidize glucose to gluconolactone during biological glucose metabolism and glucose metabolism of some bacteria such as *Aspergillus niger*. Gluconolactone can be obtained from GOx mediated reaction (refer to Figure 1.11) [86].

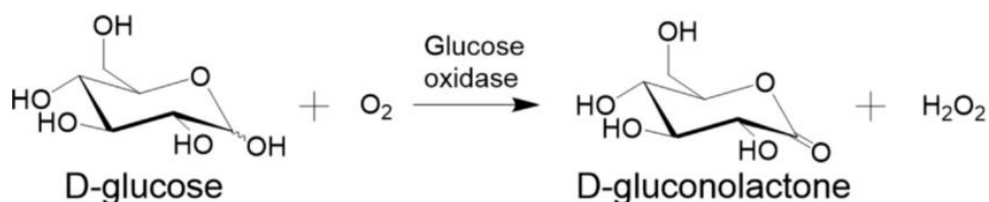


Figure 1.11: Reaction of glucose and D-gluconolactone with chemical structures [87]

1.5.2 Importance of Glucose Detection

In a healthy person, while glucose is at the level of 4.4 - 6.6 mM in the blood, the unbalanced secretion of the insulin hormone and the disruption of carbohydrate metabolism cause high blood glucose (hyperglycemia) [88]. This condition is called diabetes mellitus. There are many types of diabetes such as maturity-onset diabetes of the young (MODY), neonatal diabetes, steroid-induced diabetes, type 1 and type 2 diabetes. Among them, type 1 and type 2 have the potential for hyperglycemia, although they are managed differently [89]. Hyperglycemia can bring complications such as heart disease, blindness, and kidney failure to a level that threatens the patient's life. Monitoring the glucose level helps delay and prevent the progression of such complications [88, 90]. Proper diabetes management provides patients to regulate their lifestyle and to increase the quality of life. In this context, biosensors offer simple, cost-effective, accurate and real-time analysis [91]. Enzyme-based electrodes have several advantages in glucose detection, but enzyme immobilization is a compelling factor in miniaturized sensors. Because there is not enough active surface for enzyme immobilization, this results in weak output signals. In this line, Amara et. al. designed enzyme-based glucose sensor with aiming to enhance the number of glucose oxidase (GOx) on electrode. MWCNT and perylene-tetracarboxylic acid (PTCA) were bounded by π - π stacking. Then, nafion solution (5 %, w/w) was added into the prepared mixture. GOx was immobilized by EDC/NHS covalently. Cyclic

voltammetry method was used for detection of different glucose concentrations (1 mM to 19 mM). Produced electrode showed high sensitivity of $0.58 \mu\text{A}\text{mM}^{-1}\text{cm}^{-2}$ with a detection limit of 35 μM . The strategy developed in this study contributed to the realization of glucose measurement with a superior electrocatalytic activity by providing more electrochemical active surface area [63]. Type 2 diabetes, one of the types of diabetes, can be detected with a biomarker called non-esterified fatty acids (NEFA). In the literature, it was stated in the 1950s that NEFA detection methods were time-consuming procedures, and the measurements were not sensitive. Although better methods have been developed today, limited studies have made this field popular. In this context, Şahin et. al. developed an enzymatic biosensor for simultaneous detection of both glucose and NEFA. Nafion-glucose oxidase-Ferrocene (Nafion-GOx- Fc) was deposited on SPE for glucose detection at room temperature. Thus, GOx is entrapped in the prepared Nafion polymer solution. For the detection of NEFA, two types of enzymes (acyl-CoA oxidase and acyl-CoA synthetase) were used, and they modified on SPE layer by layer with polyDADMAC and MWCNT composite films. Results showed linear response for glucose and NEFA as 5 and 1.2 mM, respectively in human blood plasma. Results of the study highlighted the importance of glucose and NEFA in diabetes management and early diagnosis [92]. Enzyme-based point-of-care glucose sensors are frequently used in the follow-up of diabetes. Enzymes are often highly specific to target molecules but can sometimes be inactive towards the target molecule. In particular, modifications of enzymes on the electrode may reduce the bioactivity of the enzyme. Therefore, the development of non-enzyme-based biosensors has gained importance. In this context, Branagan et al. developed non-enzymatic glucose sensors with gold nanoparticles modified carbon nanotubes. This nanostructure was modified on glassy carbon. Glassy carbon electrode showed a sensitivity of $2.77 \pm 0.14 \mu\text{A}/\text{mM}$ with a LOD of 4.1 μM . Also, the produced glucose sensor showed high selectivity in the existence of fructose, ascorbic acid and galactose [93].

1.5.3 Methods for Glucose Detection

Glucose, a monomer and more complex structures (e.g. glycogen, cellulose, and starch) serves as a metabolic fuel and energy stock in most organisms and can be detected by methods such as fluorescent emission, raman scattering, colorimetric,

luminescence quenching and electrochemistry [94, 95]. Fluorescent emission method is the quantitative measurement of the amount of fluorescence with a fluorometer by stimulating the fluorescent compound as a result of enzyme activity between a substrate and enzyme. This method can be used to measure biologically important substrates such as glucose, urea and uric acid [96]. For instance, Ling et.al. developed label-free strategy for the detection of glucose. Polyethyleneimine (PEI)-capped copper nanoclusters were used as a fluorescence probe and its diameter was about 1.8 nm. In the presence of glucose, the fluorescence of the Cu nanoclusters is quenched due to the oxidation of glucose by GOx which brings out H₂O₂. Measurements were performed with this logic, and as a result of the measurements, the limit of detection for glucose was found as 8 μM in a linear range of 10–100 μM. Prepared system was also applied for the glucose detection in human serum samples [97]. Raman scattering is another glucose measurement method that can measure the energy difference between incident electromagnetic radiation and scattered electromagnetic radiation. Thus, we can get information about the frequencies and vibrational energy [98]. In this context, a surface-enhanced Raman scattering (SERS) method was used to detect glucose concentrations. For the quantitative and selective detection of glucose, 4-mercaptophenyl boronic acid (4-MPBA)-immobilized gold-silver core-shell assembled silica nanostructure was used. As a result of these measurements using the oxidase enzyme, LOD was found as 0.15 mM in the range of 0.5 to 8.0 mM. According to results, glucose can be detected in a proper physiological range [99]. Another interesting method, colorimetric measurement, is to determine the concentration of the target molecule by visual color analysis. This measurement method offers simple operation, but provides poor quantitative measurement [94]. For example, Karim et. al. developed enzyme-like structures (nanozyme) which was Ag nanoparticles, and prepared material was used for glucose detection in urine. Cotton fabric that was used in this study provided a high area of catalytically active sites and rapid absorption of glucose. LOD was obtained as 0.08 mM with a linear dynamic range of 0.1–2 mM [100]. Luminescence quenching detection technique is based on reduction in the luminescence intensity of the luminophore [101]. In a study, Chen et. al. developed a paper-based optical analytical system for sensitive, rapid and quantitative detection of glucose. Ir-Zn_e polymer was used as the luminescence sensing material. Ir-Zn_e was produced on steel mesh electrochemically and then modified on filter paper. Also, for

sensing area, GOx was immobilized in hydrogel with encapsulation, then on egg membrane. Measurement of glucose was performed simultaneously by dropping glucose on sensor. The LOD was found as 0.05 mM in a dynamic linear range of 0.05-8.0 mM. Lastly, the sensor was tested in human serum successfully [102]. However, the compelling part of these methods, exemplified above, is that they are expensive, have complex principles, and are difficult to design. Electrochemical methods are widely used in glucose sensing. On the other hand, electrochemical glucose sensors offer easy operation, low cost, more precise measurement, fast response time, portability and miniaturization [103]. Differential pulse voltammetry (DPV) is an electrochemical technique in which a pulse is periodically applied on the staircase ramp. The current difference between before and after pulse application is plotted as a function of staircase potential. This technique has become attractive because it provides a significant discrimination against charging current and is ideal for displaying the peak-shaped curve by microprocessor assisted devices [104]. DPV can detect low analyte concentrations with a higher current sensitivity than amperometry [94]. In addition, DPV provides high sensitivity and selectivity by combining the features of chronoamperometry and linear scanning voltammetry. The overlap between two oxidizable compounds with oxidation potentials of at least 50-100 mV is removed in the DPV method. Thus, oxidation of a compound produces a sharp peak rather than broad peak or plateau of linear sweep voltammetry, which is clearly visible in the DPV curve [105]. In this line, in a study using GCE modified with MWCNT and tetracynamide cobalt (II) phthalocyanine (MWCNT-CoTCIDPc), glucose was measured in a easy and sensitive manner separately by chronoamperometry and DPV. MWCNT-CoTCIDPc and GOx dropped onto GCE and dried at room temperature for 2 hours. It showed a high electrocatalytic activity and lower potential towards the oxidation of glucose via GOx. As a result of DPV measurement, LOD was obtained as 5.33 μM with a sensitivity of 3.483 $\mu\text{A}\mu\text{M}^{-1}\text{cm}^{-2}$ in a linear range of 2-12 μM . Which were better values than results of chronoamperometry measurement. Also, good selectivity in the existence of AA, DA, and UA was obtained [106]. In another study, GOx was loaded with combination of MWCNT and β cyclodextrin (β -CD) mixture. Later, this composite was chemically modified by ionic liquid on the GCE. The prepared electrode was used for the sensitive determination of glucose in honey by DPV method. As a result of the glucose measurement, the sensitivity was achieved as

35.44 $\mu\text{AmM}^{-1}\text{cm}^{-2}$ with a low LOD of 0.27 μM . Furthermore, good stability and reproducibility was obtained by the produced enzyme glucose biosensor [107]. In addition, redox mediators are of interest for electrode modification in glucose biosensors because they are successful in increasing the efficiency of electron transfer between glucose and the electrode surface. During the enzymatic reaction, an oxidized redox mediator can be reduced instead of oxygen and then re-oxidized at the electrode surface while obtaining the electrochemical signal. In this way, selective and sensitive measurement of even low glucose levels in real samples can be made. Redox mediators such as aminophenol derivatives [22], osmium complexes, ferrocene derivatives, viologens and ruthenium [108] have been used recently to improve sensor performance. In this context, Rungsawang et. al. modified SPCE with a redox mediator called 4-aminophenyl-boronic acid (4-APBA). In this study, ABPA, an aminophenol derivative, was used to improve sensor performance by reacting with the enzyme. In addition, ABPA is low cost and non-toxic. The response from this enzymatically developed electrode was 0.86 mM as the detection limit. Also, the produced electrode was tested on artificial blood serum, sweet tea, apple juice and soft drink with good accuracy [22]. Ferrocene derivatives, another redox mediator, are remarkable mediators in the development of enzymatic electrodes. In one study, an effective glucose sensor was produced by layer-by-layer modification with ferrocene, GOx, nafion and MWCNT. Ferrocene increased its electrocatalytic effect for enzymatic oxidation of glucose by acting like an electron relay between MWCNT and enzyme. This fabricated glucose biosensor worked in broad linear range (0.28 mM -14.99 mM), and it showed a small limit of detection of 8.68 μM . Furthermore, testing this sensor in human blood samples strengthened the possibility of its clinical use [109].

1.6 Aim of the Study

Screen-printing is a low cost technique suitable for large scale production of electrodes that are being used in electrochemical sensor/biosensor assemblies. The aim of the thesis was to first develop a novel acrylic varnish- and MWCNT-based conductive paste formulation and then use it to print reproducible, stable, highly sensitive, cost-effective, disposable and flexible SPCEs. To that end, the MWCNT-based paste was printed via screen-printing on a flexible substrate material (acetate) using a template prepared by a CNC machine. To improve conductivity, the reference electrode and

lower parts of the working and counter electrodes were made of silver paste. An electric tape was used to insulate the electrodes and define the detection area and contact pad. Flexible SPCEs were characterized using physical and electrochemical methods and tested for the sensitive and selective detection of DA. MWCNT-based SPCE was then modified with GOx and ferrocene methanol (FcCH₂OH) for glucose measurement. Flexible electrodes developed within the scope of the thesis are aimed to be used in a wide range of applications ranging from standard electrochemical measurements to wearable sensor technology.

Chapter 2

Material and Method

2.1 Materials

Multi-walled carbon nano tubes (MWCNT)(Outside diameter 48-78 nm)(Nanografi Nano technology, Turkey), 2K acrylic varnish (Dyo, Turkey), 2K acrylic varnish hardener (Akzonobel Kemipol Akripol, Turkey), liquid paraffin (Tekkim, Turkey), silver (Ag) paste ($\geq 99\%$)(Sigma Aldrich, USA), self-adhesive printing paper (Elçinbirlik, Turkey), acetate paper (Temat, Turkey), 405nm SLA ultraviolet (UV)-curing resin (ANYCUBIC 3D Printer Resin, China), commercial SPCE (Metroohm DropSens, Switzerland). The following chemicals were purchased from Sigma Aldrich, USA: dopamine hydrochloride (DA)($\geq 98\%$), D(+)-glucose ($\geq 99.5\%$), glucose oxidase from *Aspergillus niger* (211 U/mg), ferrocenemethanol (FcCH₂OH) (FMA) ($\geq 97\%$), phosphate-buffered saline (PBS), sodium chloride (NaCl) ($\geq 99\%$), ammonium chloride (NH₄Cl)($\geq 99.998\%$), urea ($\geq 99\%$), ascorbic acid (AA) ($\geq 99.0\%$), lactic acid ($\geq 85\%$), uric acid (UA) ($\geq 99.0\%$), acetic acid ($\geq 99\%$), sodium hydroxide (NaOH) ($\geq 98.0\%$), sucrose ($\geq 99.5\%$), mannose ($\geq 99\%$), galactose ($\geq 99\%$) and Eagle's minimal essential medium (DMEM). For the cytotoxicity test, L929 (mouse fibroblast) cell line, MTT (3-(4,5-Dimethylthiazol-2-yl)-2,5-Diphenyltetrazolium Bromide) assay, Eagle's minimal essential medium (DMEM), dimethyl sulfoxide (DMSO), penicillin streptomycin, fetal bovine serum (FBS), L-glutamine, propidium iodide, calcein AM were used.

2.2 Fabrication of MWCNT-Based SPCEs by screen printing method

As the first step of this study, templates for screen-printed electrodes were prepared. The templates were drawn in Microsoft PowerPoint program and then transferred to Laser GRBL program (Figure 2.1). Through this program, the desired shape was transferred to single-sided adhesive papers with a laser-tipped CNC machine (CNC 3018 Plus, China) at a parameter of 450 nm and output power 5.5 W. The prepared stencils were adhered on acetate paper.

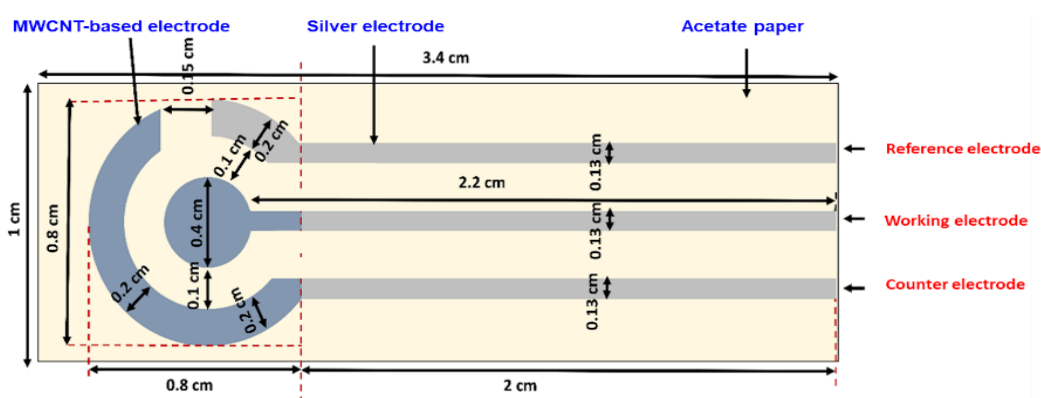


Figure 2.1: The design shows the dimensions used in the production of the screen-printed electrode and its components

Then, MWCNT-based pastes were prepared by mixing MWCNT powder (4.6 mg, 9.2 mg, 18.4 mg, 36.8 mg), 250 μL of varnish, 125 μL of varnish hardener and 20 μL of paraffin for 5-6 minutes. The obtained pastes were applied to the upper parts of the WE and counter electrode (CE) on the stencil with the help of a spatula, and electrodes with different MWCNT ratios were obtained. It was left to dry at room temperature for 4 hours, and after drying of the paste, electrode surface was sanded to obtain a smooth surface. Then, the lower connection parts of the triple electrode system and the reference electrode were printed with commercial silver paste with the help of a spatula. A hair dryer was applied for 20 minutes to dry the silver paste. The adhesive stencil was then gently removed from the acetate paper and proceeded to the next step.

In order to isolate the connection part of the electrodes and to determine the sensing area, the electrical tape was cut in a specific structure with a laser-tipped CNC machine. The prepared tape was adhered to the relevant part of the electrode. Finally, acetate paper on which the electrodes were printed was cut to a length of 3.4 cm and a width of 1 cm. In order to optimize the MWCNT ratio in the paste, 5 different electrodes with different MWCNT ratios (11.5, 23, 92 and 184 g/L) were produced.

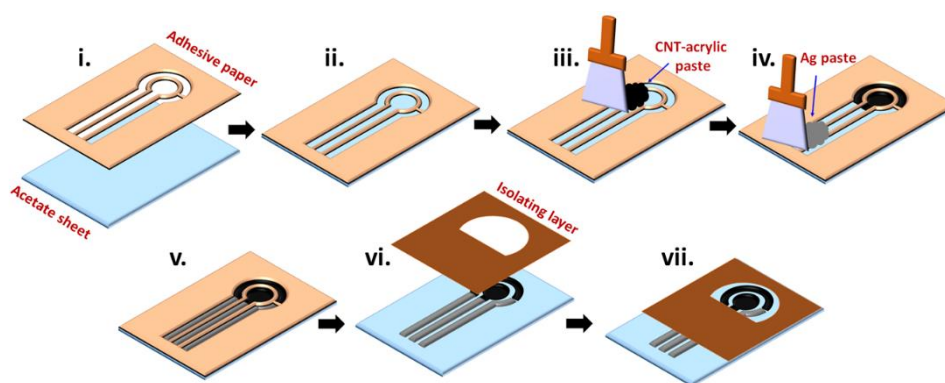


Figure 2.2: Fabrication steps of the MWCNT/SPE using screen printing

2.3 Electrochemical Characterization

All electrochemical measurements and characterizations of fabricated flexible SPCE were performed at room temperature in a Faraday cage with a potentiostat (Autolab PGSTAT204, Metrohm, Switzerland) with a connector (Figure 2.3c and Figure 2.3d). Cyclic voltammetry (CV) and differential pulse voltammetry (DPV) measurements were carried out. For optimizing the MWCNT ratio, CV measurements of prepared MWCNT electrodes (11.5, 23, 92 and 184 g/L) were performed by sweeping the potential between 0 and +0.4 V (vs. Ag/AgCl) at a scan rate (ν) of 50 mVs^{-1} in 1mM FcCH₂OH containing PBS solution. All remaining measurements and work with the selected electrode (92 g/L) have been completed. EIS measurements were performed on open circuit potential with 10 mV in frequency range of 10 Hz to 10 kHz. In EIS measurement, 5mM Fe(CN)₆^{-3/4} in 0.1 M potassium chloride (KCl) solution was used as electrolyte and Randles circuit model was used for Rct analysis. EIS data was adapted to the circuit using AUTOLAB 302 Nova 2.1.5 software.

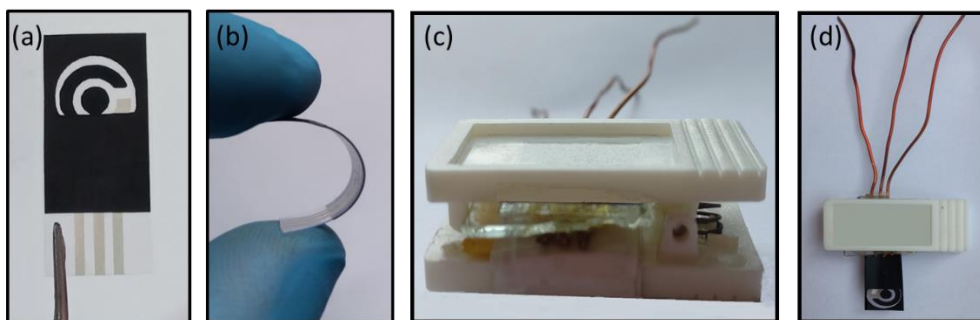


Figure 2.3: Flexible SPE (a), bent SPE (b), side view of the developed SPE connector (c) and front view of SPE connector and SPE (d)

To demonstrate the electrochemical transfer behavior of the chosen electrode, CV measurement was made by sweeping the potential between 0 V- 0.4 V (vs. Ag/AgCl) at different scan rates of 5, 10, 25, 50, 75, 100, 150, 200, 250 and 500 mV/s in FMA solution. Different scan rates were carried out to study the relationship between peak-to-peak potential separation (ΔE_p) and $v^{-1/2}$. Furthermore, bending test was performed for investigation of flexibility of the electrode. The electrochemical behavior of the initial state of the electrode was examined by CV measurement. Then, the electrode was bent 180° 100 times and its electrochemical behavior was observed by CV measurement after every 10 cycles (Figure 2.3b). CV measurements for the bending test were made in 1 mM FMA solution between 0 and 0.4 V (vs. Ag/AgCl). Additionally, a stability test was performed with flexible SPCE. CV measurement of one electrode was taken on different days (1st, 3rd, 5th, 7th, 10th and 15th days) by sweeping the potential between 0 and +0.4 V (vs. Ag/AgCl). In addition to the above-mentioned studies, reproducibility of the flexible SPCE was tested by taking the CV measurement of the 3 different electrode from the same batch. CV measurements were performed by the same parameter as above-mentioned. Thus, electrochemical characterization part was completed.

2.4 Dopamine Detection

In order to examine the dopamine sensing behavior of the flexible SPCE, chronoamperometry method was carried out. Chronoamperometry measurements were taken by applying a constant voltage of +0.3 V (Ag/AgCl) for 90 sec. Electrode

was immersed in DA containing PBS solutions (0, 5, 10, 50, 100 and 200 μM). The obtained current values were used to draw a calibration curve and calculate the limit-of-detection (LOD) ($\text{LOD} = 3.3 \cdot \sigma_s^{-1}$) along with the sensitivity.

2.5 SPCE-Based Glucose Biosensor

At this step of the study, flexible SPCE was modified with FcCH_2OH and glucose oxidase (GOx) to prepare enzymatic glucose biosensor. In this line, working electrode of the sensor was modified with 2 μl FMA (10 mM), 2 μl GOx (4kU/ml), 2 μl FMA (10 mM), 2 μl GOx (4kU/ml) and 4 μl FMA (10 mM), respectively. Electrode was left to dry for each modification. As the final step of the modification, 0.5 μL of UV-resin was dropped onto WE and the surface was cured through 210 sec exposed to 450 nm UV light using OmniCure S2000 Spot UV curing system (320 nm-500 nm).

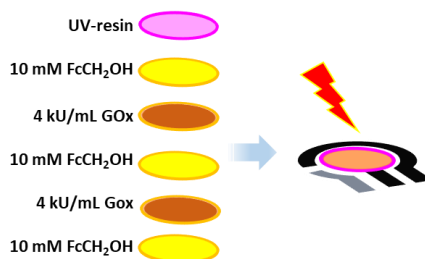


Figure 2.4: Modification steps of flexible glucose biosensor

Detection of glucose was achieved by DPV at different molarities (0, 0.05, 0.1, 0.25, 0.5, 1, 2.5, 5 mM) in artificial sweat. Artificial sweat solution was prepared by mixing 5 g L^{-1} urea, 17.5 g L^{-1} NH_4Cl , 20 g L^{-1} NaCl , acetic acid (0.25%), lactic acid (0.088%) in distilled H_2O [110]. Additionally, the pH of the artificial sweat was adjusted to 6.3 with NaOH . DPV measurement was done by changing the potential between 0 and +0.6 V (vs. Ag/AgCl) at amplitude of 50 mV. Calculation of the LOD ($\text{LOD} = 3.3 \cdot \sigma_s^{-1}$) along with the sensitivity was made with the help of peak current values of the DPV graphs.

2.6 Selectivity Test

Selectivity tests of both DA electrode and glucose biosensor were performed. Firstly, selectivity of the bare electrode against dopamine was tested. The test was made using chronoamperometry in the existence of UA and AA. In more detailed, a constant current value at a stable potential of +0.2 V (versus Ag/AgCl) was first obtained in PBS, and then 100 μ M DA, 100 μ M ascorbic acid and uric acid separately, finally, 200 μ M DA solution were added. Thus, the electrochemical response of flexible SPCE against dopamine was monitored over time.

In the next step, the selectivity of the GOx modified glucose biosensor against glucose was tested. The test was carried out using chronoamperometry in the presence of several interferents (sucrose, mannose, galactose and urea) in artificial sweat. Briefly, a stable current value at a constant potential of +0.3 V (versus Ag/AgCl) was first obtained in artificial sweat, and then 5 mM glucose, 10 mM sucrose, 10 mM mannose, 10 mM galactose, 10 mM urea and once again 5 mM glucose were added respectively. Thus, the electrochemical response of the flexible SPCE glucose biosensor against glucose detection was monitored depending on time.

2.7 Cytotoxicity

For the last part of the study, L929 (mouse fibroblast) cells were used for the cytotoxicity test [111]. For the preparation of medium, 56.81 mL FBS, 5.7 mL L-glutamine, and 5.7 mL penicillin streptomycin was added inside of 500 mL of DMEM. 25 cm² flasks were used for culturing the cells. Then, L929 cells were passaged twice. Then, cells were seeded into two different 24-well plates. For the MTT assay, twelve wells of one well-plate were used for three different samples, and three of them were used for the control group. There were 2×10^4 cells for each well [112]. It was aimed to observe whether there is toxic substance release or not, by keeping 4 samples from 3 different samples, 12 samples in total, with 1 mL of medium in each well, in a 24 well-

plate for 24 hours (Figure 2.5). After 24 hours, the medium in the wells and samples were discarded.

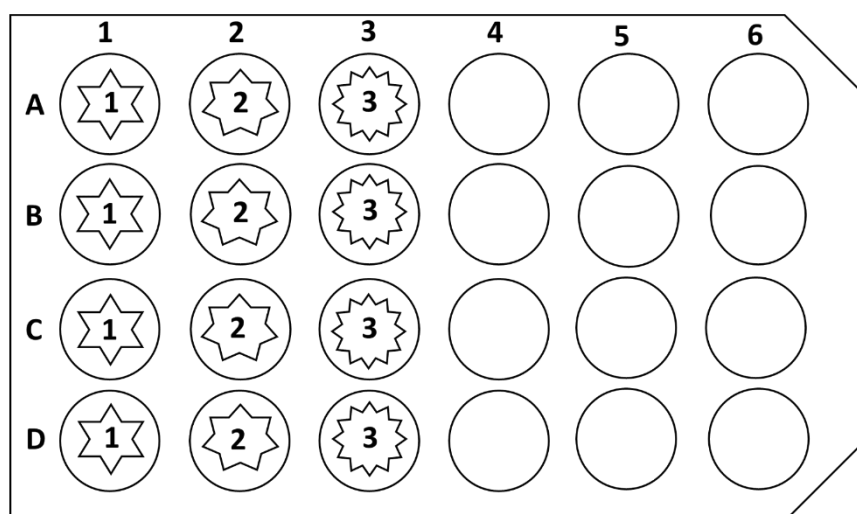


Figure 2.5: Experimental setup for the 3 different samples (1=acetate paper, 2=MWCNT/SPE, 3=flexible glucose biosensor)

Then, 1 mL of a mixture of 90 % DMEM (Eagle's minimal essential medium) and 10 % MTT solution (5 mg/mL) was added to each cell seeded well. After being kept in the incubator for two hours, the media in each well was discarded. Then, we put 1 mL of DMSO (dimethyl sulfoxide) in each well and quickly mixed the wells in the shaker. Two minutes later, MTT datas were acquired at a wavelength of 575 nm by a multi-mode plate reader (Synergy Mx, BioTek, USA). For imaging living and dead cells, three wells of one well-plate were used for three different samples. There were 2×10^4 cells for each well. It was aimed to image whether there are living cells or not, by keeping 3 different samples with 1 mL of medium in each well, in a 24 well-plate for 24 hours. After 24 hours, the medium in the wells and samples were discarded. Then, for imaging the dead cells, 1.5 μ L propidium iodide and for imaging the living cells, 1.5 μ L calcein AM were dissolved in 600 μ L PBS. 200 μ L of the prepared mixture was added to each well. Half an hour after this procedure, images were taken under a fluorescent microscope (ZEISS Axio microscope) [113].

Chapter 3

Results and Discussion

3.1 Fabrication of MWCNT-Based SPCE

Screen printing stencil was designed for the fabrication of MWCNT/SPCE. In the produced design, a triple electrode system was prepared. The stencil was used to fabricate a triple electrode system on acetate paper by screen printing method (Figure 2.2). As can be easily seen in Figure 2.3a, flexible SPEs were successfully printed. In this study, a conductive paste based on MWCNT was prepared. The MWCNT concentration of the prepared paste had a serious effect on both its physical and electrochemical properties. To see that effect, the composition of the conductive paste was first optimized to determine the optimum concentration for easy printing and acceptable electrochemical behavior. Accordingly, flexible SPEs made of conductive pastes with varying MWCNT concentrations were prepared and electrochemically tested in PBS solution containing 1 mM FcCH_2OH using the CV method. The smaller the peak-to-peak potential separation (ΔE_p) according to the CV method, the better the electrochemical reversibility. Also, the small ΔE_p symbolizes improved electron transfer efficiency. As seen in Figure 3.1a, ΔE_p decreased from 281 mV to 82 mV when the MWCNT concentration increased from 11.5 to 92 g L⁻¹. MWCNT/SPCE with a concentration of 184 g L⁻¹ MWCNT showed ΔE_p as 96 mV, which may be due to the surface morphology of the SPE as the prepared paste is highly viscous. In contrast to the 184 g L⁻¹ concentration level, 92 g L⁻¹ provided easy administration and lower ΔE_p , so 92 g L⁻¹ was chosen and used as the ideal concentration level for further

experiments. MWCNTs have high Young's modulus, strength, flexibility and unique geometry [39]. To understand the contribution of MWCNTs to the flexibility of the fabricated electrode and to evaluate its effect on the electrochemical response, an SPE 180° was bent 70 times and CV curves of the electrode were obtained in 1 mM FcCH₂OH for comparison after every 10 bending cycles. Figure 3.1b shows the FcCH₂OH oxidation (anodic peak current, $I_{p,a}$) and reduction peak currents (cathodic peak current, $I_{p,c}$) of each 10 bending cycle. The average $I_{p,a}$ ($n = 3$) remained almost the same after 30 bending cycles and increased 8.6 % following 70 times of bending. However, student's t-test showed no significant change in both $I_{p,a}$ and $I_{p,c}$ after 70 times of bending ($p > 0.05$), proving that the SPEs are flexible enough to withstand such physical deformations and maintain their electrochemical response without significant change. A similar trend was observed with the reduction currents.

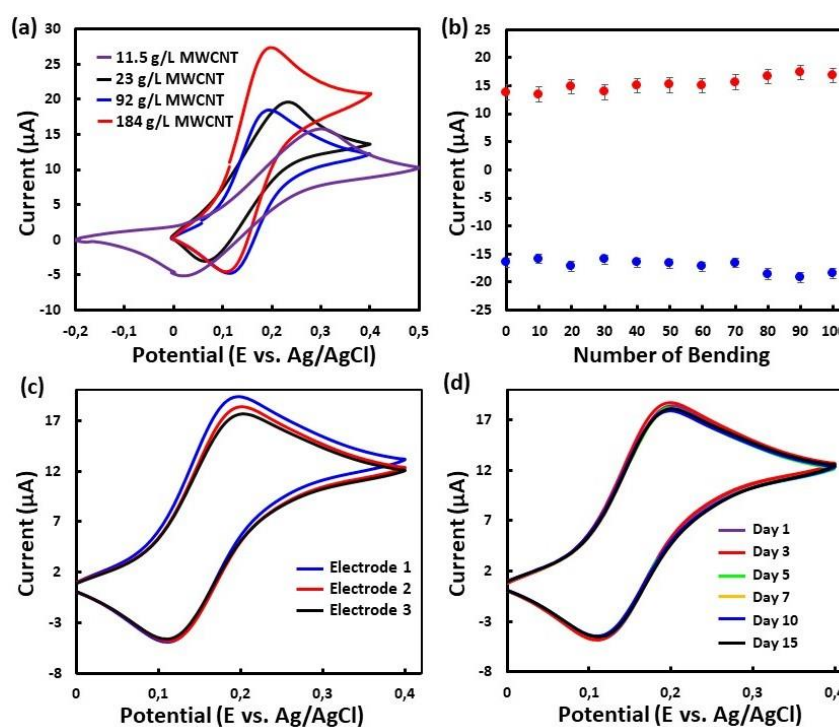


Figure 3.1: CV curves of SPE electrodes fabricated with different amounts of MWCNT (a), $I_{p,a}$ and $I_{p,c}$ of an SPE in FcCH₂OH after every 10 cycles for a total of 100 cycles of bending test (b), CV curves from three different SPE electrodes (c), and one SPE over 15 days (d)

In order to demonstrate the consistency of electrodes, a reproducibility test was performed, where the CV curves of three different electrodes were obtained in 1mM FcCH₂OH (Figure 3.1c). The relative standard deviation (RSD) values calculated using $I_{p,a}$ and $I_{p,c}$ were 4.59 % and 3.86 %, respectively, proving the high reproducibility of the proposed fabrication approach. Furthermore, to investigate stability of the electrode, the CV curves of an SPE were taken daily for a total of 15 days. Both $I_{p,a}$ and $I_{p,c}$ remained nearly the same with an RSD values of 5.09 % and 3.67 %, respectively, indicating that the SPE had a highly stable response and could be used repeatedly (refer to Figure 3.1d). In recent years, the use of flexible substrates such as kapton, PET, paper, textile, acetate paper has led to the development of implantable biomedical sensing devices, flexible solar cells, flexible pressure and chemical sensors. The biggest challenge in this trend is not only their manufacture but also the stability of these devices in terms of electrochemical, mechanical, and electrical properties [114]. In this context, in a study, a carbon microelectrode was developed. The stability test of the produced electrode was carried out for a period of 5 days and the measurements were recorded with SWV. As a result, the long-term stability of the flexible electrode was evaluated electrochemically and showed nearly identical current responses [115].

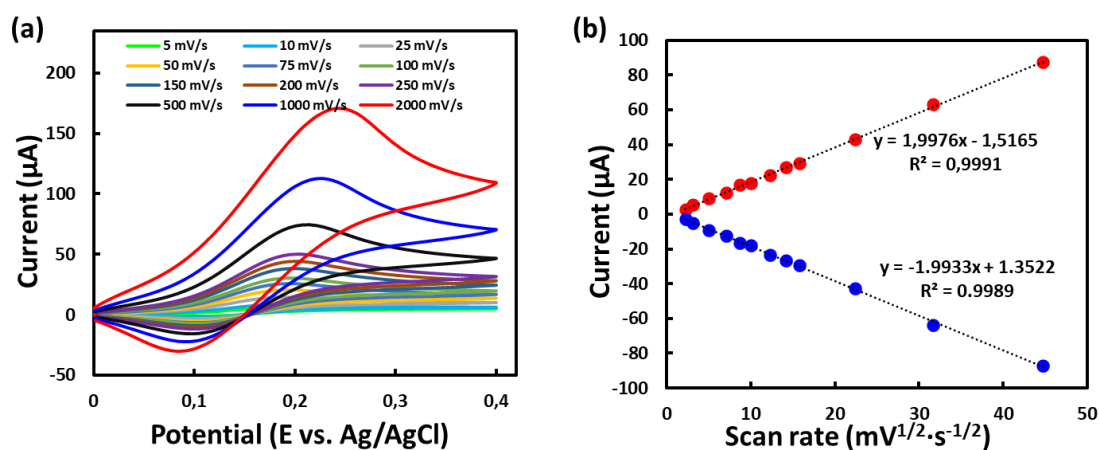


Figure 3.2: Graph shows that curves at scan rates ranging from 5 to 2000 mVs⁻¹ obtained by CV technique (a) and a graph showing the relationship between scan rate and $I_{p,a} - I_{p,c}$ (b)

The ΔE_p and $I_{p,a} - I_{p,c}$ can help to give information about reversibility of the electrochemical system. Thus, in order to analyze the influence of scan rate variation on ΔE_p , the electrode reaction and $I_{p,a} - I_{p,c}$ of FcCH₂OH was investigated by obtaining CV curves at different scan rates in a range of 5 to 500 mVs⁻¹. It can be verified that the wave is reversible by looking at the separation of the anodic and cathodic peaks. If they are much further apart from each other, it may indicate that the wave is not reversible, the solution resistance is not properly balanced. In addition, the constant E_p at varying scan rates indicates that the reaction is reversible. In this study, according to the CV curves in Figure 3.2a, ΔE_p remained almost the same and $I_{p,a} - I_{p,c}$ increased with increasing scan rate. The relationship between $I_{p,a} - I_{p,c}$ and $v^{-1/2}$ displayed an excellent linearity with almost the same R^2 value of 0.998 (Figure 3.2b), suggesting a diffusion-controlled electrode reaction [116]. The $I_{p,a} / I_{p,c}$ ratio was calculated to be 1.004, also confirming the electrochemical reversibility of the redox mediator FcCH₂OH at the surface of the flexible MWCNT-based SPE [117]. EIS plots were performed on open circuit potential with 10 mV in frequency range of 10 Hz to 10 kHz. In EIS measurement, 5mM Fe(CN)₆^{-3/4} in 0.1 M potassium chloride (KCl) solution was used as electrolyte and Randles circuit model was used for R_{ct} analysis. EIS data was adapted to the circuit using AUTOLAB 302 Nova 2.1.5 software. Consistent with CV results, the EIS result showed a low R_{ct} value (347 Ω) as shown in Figure 3.3a and thus a high electron transfer rate at the surface of electrode. Calculated R_{ct} was measured considerably lower than that of a commercially available SPE (1.92 k Ω).

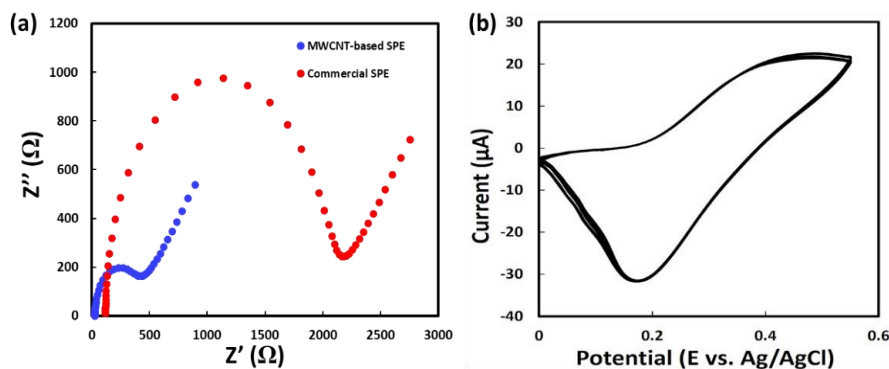


Figure 3.3: The EIS curve of the bare MWCNT-based and commercial SPE in 5 mM Fe(CN)₆^{-3/4} (a) and multiple CV curves of the SPE glucose biosensor in 1 mM FcCH₂OH (b)

3.2 Surface Characterization

Scanning electron microscope (Carl Zeiss 300VP SEM Device) was used for surface characterization of MWCNT/SPCE. Before SEM images were taken, the samples were coated with a gold coater (QUORUM Q150 RES) with a gold layer of 8-10 nm thickness. Before and after a bending test, the surface of an SPE was imaged using SEM, which showed that the printed electrodes had a relatively smooth surface and did not experience any observable damage, as shown in Figure 3.4a and Figure 3.4c. SEM images showed network-like structures originating from MWCNT on electrode surface. Flexible SPE surface showed a micro-/nano-porous network morphology providing a large surface-to-volume ratio, which is important especially for biosensor applications (Figure 3.4b and Figure 3.4d). In the light of the results, it is highly likely to fabricate such electrodes in much smaller sizes using the proposed fabrication approach.

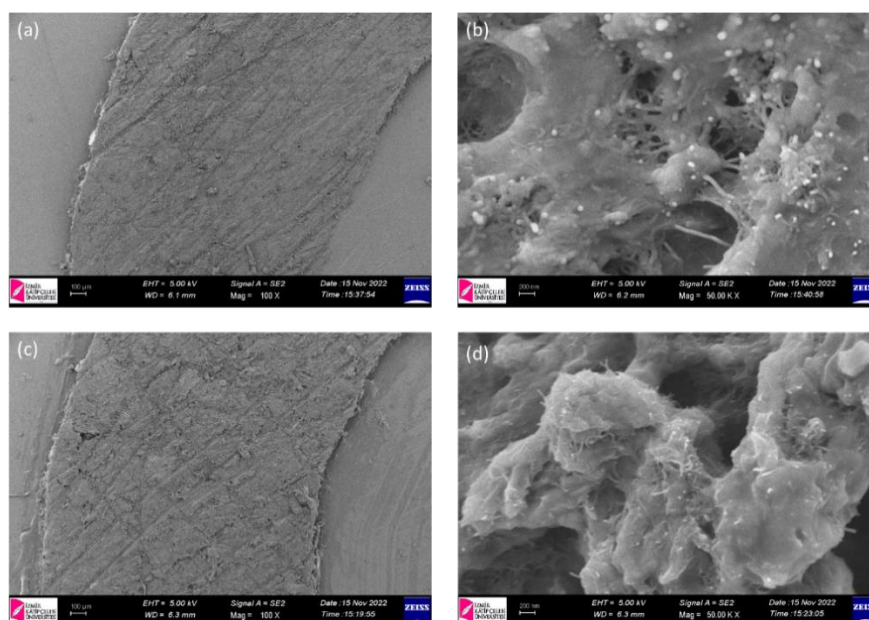


Figure 3.4: SEM images of an electrode before bending (a and b) and after bending (c and d) at 100 μm and 200 nm

3.3 Dopamine Detection

In this part of the study, following physical and electrochemical characterization, flexible MWCNT-based SPE was used for the detection of dopamine (DA). Chronoamperometry was used at a constant potential of +0.3 V (vs. Ag/AgCl) to oxidize dopamine at varying concentrations. The *i*-*t* curves shown in Figure 3.5a displayed a DA concentration dependent response. A calibration curve was drawn by using the $I_{p,a}$ of DA at 90 sec for each concentration level (Figure 3.5b). According to the results, the electrode showed good linear response towards dopamine with an R^2 value of 0.993 (in the range of 5 to 500 μM). LOD and sensitivity of electrode ($n=3$) were obtained as 0.87 μM and 0.0905 $\mu\text{A}\mu\text{M}^{-1}\text{cm}^{-2}$, respectively.

Table 3.1: Comparison of analytical performance of SPE-based dopamine sensors

Electrode Type	Sensitivity ($\mu\text{A}/\mu\text{M}\cdot\text{cm}^2$)	LOD (μM)	Linear Range (μM)	Reference
FTO/MoS2/SPE	0.05	0.246	1-300	[118]
AuNS/SPE	0.000056	0.33	0.2-50	[119]
Ti ₃ C ₂ /SPE	0.0458	0.15	0.5-600	[120]
RGO/PNR/AuNP/SPE	0.01338	0.17	0.57-500	[121]
ERGNRs/SPE	0.0549	0.15	0.5-300	[122]
PEDOT: PSS/RGO/SPE	0.0249	-	12.5-100	[123]
Flexible MWCNT-SPE	0.0905	0.87	5-500	This work

Compared to some recently published studies with SPE [124-127] (Table 3.1), the present flexible MWCNT-based SPE displayed comparable or low detection limit and broader linear range mostly because of a large surface-to-volume ratio and good mass transport ability provided by the MWCNTs and micro-/nano-porous network morphology (Figure 3.4) [128].

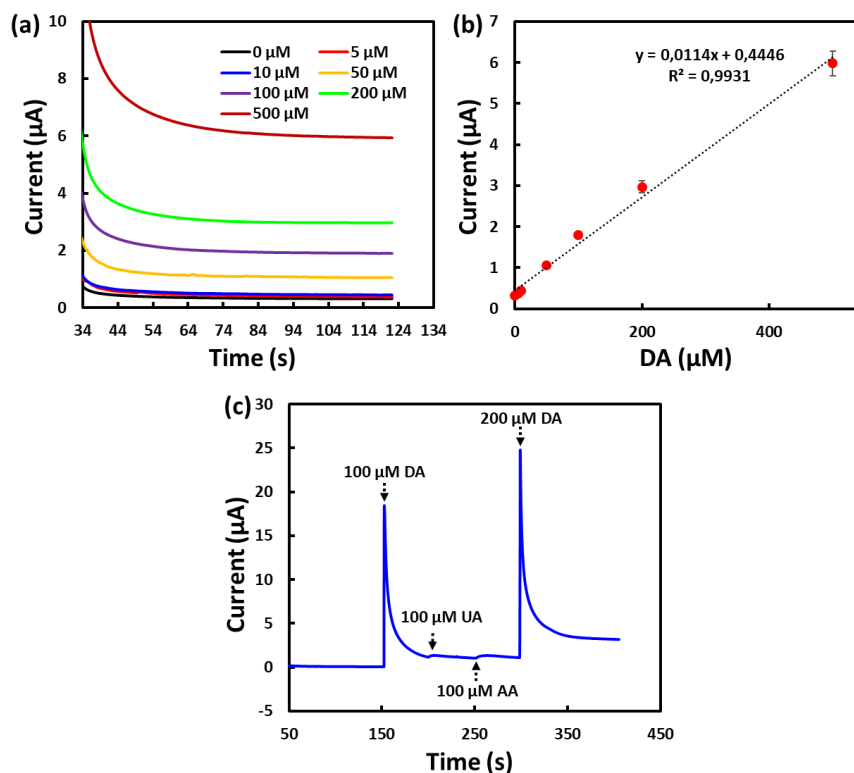


Figure 3.5: Chronoamperometric curves obtained in PBS containing dopamine in the range of 0 to 500 μM (a) together with a calibration curve (b) and selectivity results at 0.3 V (vs. Ag/AgCl) (c)

3.4 SPCE-Based Glucose Biosensor

Flexible MWCNT-based SPE was utilized for the glucose detection. At first, a biosensor was fabricated by modifying the surface of a flexible MWCNT-based SPE to detect glucose in artificial sweat based on electrochemical-enzymatic redox cycling. Figure 2.4 shows modification of GOx and FcCH₂OH layer by layer on the electrode surface and finally the surface was coated with a UV-curing resin to trap the chemicals. The redox cycle mechanism starts with the oxidation of FMA to FMA⁺, while the glucose of GOx catalyzes β -D-glucose to D-glucono1,5-lactone (Figure 3.6). Later, redox cycling of FcCH₂OH between GOx and the electrode causes an amplification in the FcCH₂OH I_{p,a}, which can be directly associated with the glucose concentration and can be sensed by electrode.

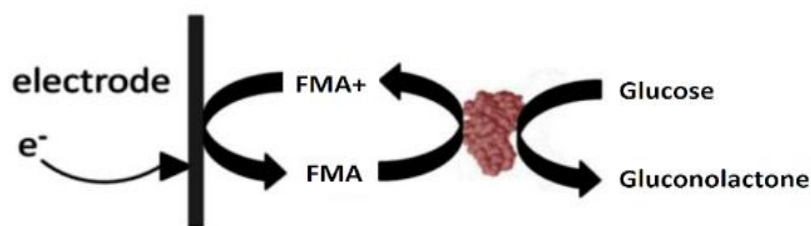


Figure 3.6: Electrochemical mechanism in glucose detection using a redox mediator

First, CV curves of the biosensor was repeatedly recorded to confirm that the chemicals do not leak out of the resin (Figure 3.3b). Both the $I_{p,a}$ and $I_{p,c}$ did not change significantly after 20 repeats of CV, proving that the detection strategy can be safely used. Afterward, the biosensor was tested for electrochemical detection of glucose at varying concentrations using DPV (Figure 3.7a). As seen in Figure 3.7b, DPV signals increased proportionally and exhibited a concentration dependent response. The biosensor showed a linear response especially up to 1 mM with an R^2 value of 0.992. The LOD and sensitivity of the electrode ($n=3$) were calculated to be $31.7 \mu\text{M}$ and $47.647 \mu\text{AmM}^{-1}\text{cm}^{-2}$, respectively. Sweat glucose level has been well correlated with blood glucose [129, 130] and its physiological level in sweat for healthy humans and diabetic patients is in the range of about 60 to $110 \mu\text{M}$ and 10 to $1000 \mu\text{M}$, respectively [131]. Considering the LOD, it can be concluded that the current flexible biosensor has great potential for non-invasive glucose detection, especially in diabetic patients.

Table 3.2: Comparison of analytical performance of SPE-based glucose biosensors

Electrode Type	Sensitivity ($\mu\text{A}/\text{mM}\cdot\text{cm}^2$)	LOD (μM)	Linear Range (mM)	Reference
Gox/GO/Au/SPE	3.1732	319.4	3-9	[62]
CHI/GO _x /APTES/1.5% MWCNT-dPIn/SPE	182.9	10	0.01-100	[132]
MWCNT/PTCA/Nf/GO _x /S PE	0.58	35	1-19	[63]
ABPA/Py/SPE-Pt	-	336.5	1.11-44.4	[133]
AuNp/MWCNT/SPCE	2.77	4.1	0.1-25	[93]
rGO/AuNPs-Gox/DHB/SPE	-	630	1-11	[134]
PB/PANI/Gox/SPE	16.66	-	0-12	[135]
PAA/GO _x -CNT/Pt-SPE	34.1	10	0-5	[136]
Pt/rGO/P3ABA/GO _x /SPE	22.01	44.3	0.25-6	[137]
MWCNT- COOH/CHI/GO _x /PB/SPE	-	40.36	0-11.5	[138]
Flexible FcCH₂OH/GO_x/MWCNT- SPE	47.647	31.7	0-1	This work

Some of the recent reports which studied on electrochemical detection of glucose by SPEs were studied, and the performance of the biosensor was compared with these reports in terms of sensitivity and LOD (Table 3.2). It seems that the present biosensor showed a comparable or better performance than most of these biosensors.

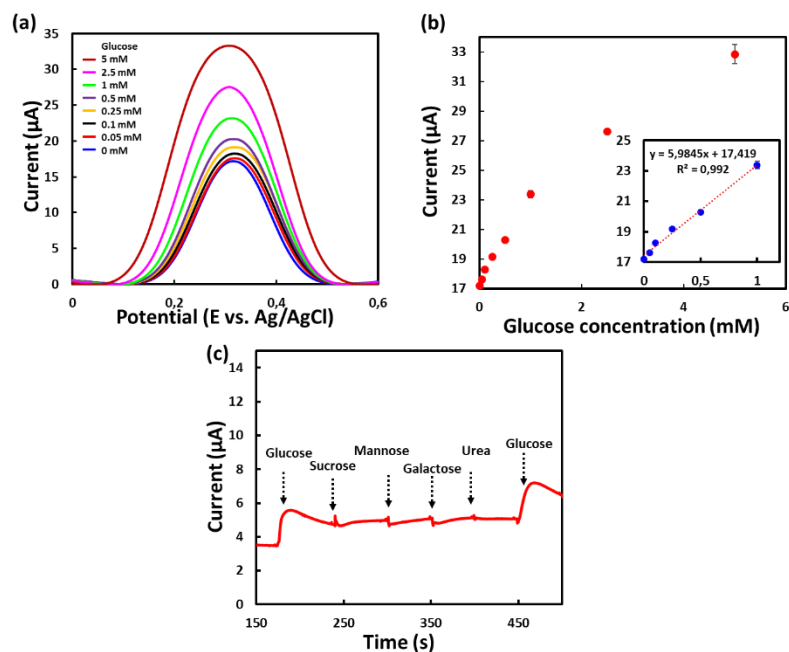


Figure 3.7: DPV curves obtained in artificial sweat containing varying concentrations of glucose (a) together with a calibration curve (b) and glucose selectivity results at 0.3 V (vs. Ag/AgCl) (c)

3.5 Selectivity Test

Selectivity of the electrode for dopamine was also tested against uric acid and ascorbic acid using chronoamperometry. According to the result given in Figure 3.5c, the $I_{p,a}$ increased proportionally when DA was added to PBS, but the same response was not observed with the interferents, confirming the high selectivity of SPE for DA at +0.3 V (vs. Ag/AgCl). Distinguishing DA and UA is hard due to the small potential difference between their oxidation peaks. Selective detection of both is required [68]. In this study, highly selective detection of dopamine was demonstrated.

Lastly, the selectivity of the flexible glucose biosensor was tested against various interfering species. As can be seen in Figure 3.7c, the addition of glucose resulted in an abrupt increase in the $I_{p,a}$, while the addition of other species at higher concentration did not cause a significant change in the response, manifesting high selectivity of the biosensor for glucose.

3.6 Cytotoxicity

The biosensor was fabricated by modifying the surface of a flexible MWCNT-based SPE to detect glucose in artificial sweat based on electrochemical-enzymatic redox cycling. The produced electrode should be noted that acrylic varnish is non-toxic after curing and therefore the present SPEs are suitable for non-invasive health monitoring. For this purpose, cytotoxicity test was performed by using L929 cells for in vitro test. Since the electrode is produced for single use, unlike other studies, no long-term cytotoxicity test was performed, only a 24-h cytotoxicity test was performed. MTT assay tests were carried out to check the cytotoxicity of the produced electrodes. Checking of toxicity of the electrodes was performed by incubating the electrodes with L929 cell culture for 24 h. The media was collected, and a MTT assay performed to check the cytotoxicity. As shown in Figure 3.8a, the L929 cells remained viable in the presence of bare MWCNT/SPE, but cell viability was decreased in the presence of glucose biosensor. This situation was investigated by performing individual cytotoxicity testing of the building blocks of the glucose biosensor. As a result, it was found that the reason for the toxicity of the glucose biosensor was the UV resin. In this study, a relatively inexpensive UV resin was used to capture the chemicals on the electrode surface. Instead of UV resin, more costly but biocompatible materials with the same purpose can be used. For example, poly (3,4-ethylenedioxythiophene) (PEDOT), is a conductive polymer that can be used as a coat in sensors due to its electrical conductivity, its stability, and biocompatibility. A conductive polymer can allow the immobilization of biologically active materials and can help to direct molecules to the specific binding between biomaterials [139]. Apart from this, polymeric materials such as nafion, cellulose acetate, electropolymerized films (e.g., polyphenol) and a multilayer mixture of these polymers can provide biocompatibility, permselective films and mechanical stability to enzymes against denaturalization [65], while at the same time they provide enzyme encapsulation on the electrode surface and electrical conduction [140]. As shown in Figure 3.8b, cell viability was observed in 24 h, for obtaining the graph, data on the graph was expressed as means with standard deviations (mean \pm SD) [112]. Also, statistical significance was obtained by the student t test, and was set at level of $p < 0.05$ when compared with the control group [113]. Results indicated that MWCNT and acrylic varnish are biocompatible as stated.

In conclusion, the bare electrode is biocompatible, but glucose biosensor is not biocompatible, so the top layer of the biosensor should be changed with more biocompatible material.

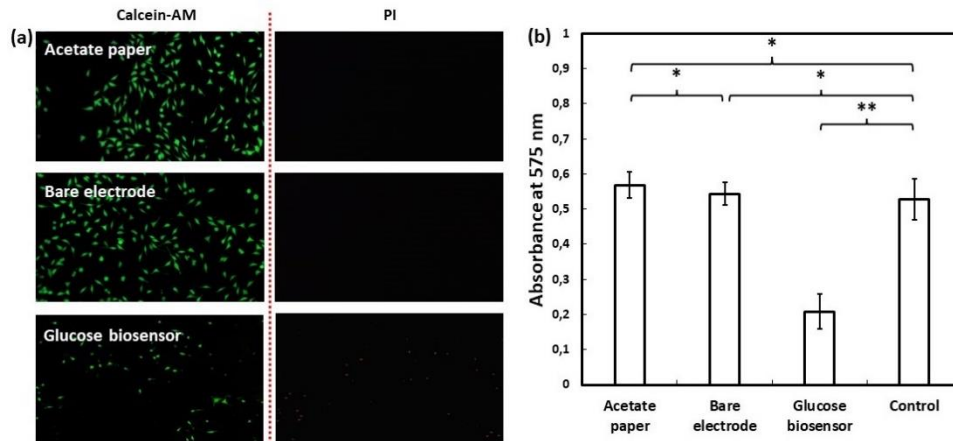


Figure 3.8: Cytotoxicity study of flexible MWCNT-based SPE. Fluorescent images of the dyed viable (green) and dead (red) cells for an acetate paper, flexible MWCNT-based dopamine sensor (bare electrode), flexible MWCNT-based glucose biosensor after 24 hour submersion (a), cell viability of L929 cells by MTT assay after 24 hour submersion (b)

Chapter 4

Conclusion

In this study, a novel acrylic varnish and MWCNT-based conductive paste formulation was first developed to print flexible SPEs via a CNC-made stencil and then applied for the electrochemical detection of DA and sweat glucose. Mostly because of the excellent adhesion properties of the acrylic varnish, the SPE showed a stable response after being subjected to multiple bending stress, confirming its flexibility and mechanical strength. The low RSD (%) values calculated based on $I_{p,a} - I_{p,c}$ of the three individual SPEs proved the reproducibility of the fabrication approach. Furthermore, stable response over two weeks indicated that SPEs could be used multiple times and applied to long-term measurements. In other words, the SPEs offered the advantages of predictable rapid electrochemical response, flexibility, portability as well as low-cost manufacturing. The electrochemical detection performance of the SPEs was first tested with DA and then glucose. Bare SPEs were utilized for dopamine detection, and they showed a great performance in both sensitivity and selectivity mostly thanks to large surface-to-volume ratio provided by MWCNTs and micro-/nano-porous network morphology. Considering the potential application in wearable sensor technology, a biosensor was made using SPE to detect glucose at varying concentrations in artificial sweat based on electrochemical enzymatic redox cycling. According to the results, the flexible SPE-based glucose biosensor displayed a remarkable performance and linear response in the physiological range especially in diabetic patients, suggesting that the glucose biosensor has great potential for non-invasive health and/or practical fitness monitoring applications.

References

- [1] Suryasa IW, Rodríguez-Gómez M, Koldoris T. Health and treatment of diabetes mellitus. *International Journal of Health Sciences* 2021; 5(1): i-v. doi.org/10.53730/ijhs.v5n1.2864
- [2] Baharuddin NA, Abdul Rahman NF, Abdul Rahman H, Somalu MR, Azmi MA. Fabrication of high-quality electrode films for solid oxide fuel cell by screen printing: A review on important processing parameters. *International Journal of Energy Research* 2020; 44(11): 8296-8313. doi.org/10.1002/er.5518
- [3] Metters JP, Kadara RO, Banks CE. New directions in screen printed electroanalytical sensors: an overview of recent developments. *Analyst* 2011; 136(6): 1067-1076. doi.org/10.1039/C0AN00894J
- [4] Wang D, Zhang Y, Lu X, Ma Z, Xie C. Chemical formation of soft metal electrodes for flexible and wearable electronics. *Chemical Society Reviews* 2018; 47(12): 4611-4641. doi.org/10.1039/C7CS00192D
- [5] Van Hazendonk LS, Pinto AM, Arapov K, Pillai N, Beurskens MR, Teunissen J-P, *et al.* Printed Stretchable Graphene Conductors for Wearable Technology. *Chemistry of Materials* 2022; 34(17): 8031-8042. doi.org/10.1021/acs.chemmater.2c02007
- [6] Tao X.(Ed.) *Wearable electronics and photonics*, 1st ed. Elsevier; 2005.
- [7] Pillai AS, Chandran A, Peethambharan SK. MWCNT Ink with PEDOT: PSS as a multifunctional additive for energy efficient flexible heating applications. *Applied Materials Today* 2021; 23 100987. doi.org/10.1016/j.apmt.2021.100987
- [8] Cazac-Scobioala V, Cîrja J, Bălan EM, Mohora C. The study of the screen printing quality depending on the surface to be printed. *Proceedings of the*

MATEC Web of Conferences; 2018 February 15; Chişinău, Moldova. EDP Sciences; 2022. 1-6.

- [9] Riemer DE. The theoretical fundamentals of the screen printing process. *Microelectronics International* 1989; 6(1): 8-17. doi.org/10.1108/eb044350
- [10] Herrasti Z, Serna Edl, Ruiz-Vega G, Baldrich E. Developing enhanced magnetoimmunosensors based on low-cost screen-printed electrode devices. *Reviews in Analytical Chemistry* 2016; 35(2): 53-85. doi.org/10.1515/revac-2016-0004
- [11] Şen M. Flexible Screen-printed MWCNT-based Electrodes. *Proceedings of the 2nd International Conference on Engineering and Applied Natural Sciences; 2022 October 15-18; Konya, Türkiye. 802-805. https://www.iceans.com/iceans2022.*
- [12] Topsoy OK, Muhammad F, Kolak S, Ulu A, Güngör Ö, Şimşek M, *et al.* Fabrication of electrospun polycaprolactone/chitosan nanofiber-modified screen-printed electrode for highly sensitive detection of diazinon in food analysis. *Measurement* 2022; 187 110250. doi.org/10.1016/j.measurement.2021.110250
- [13] Zoerner A, Oertel S, Jank MP, Frey L, Langenstein B. Human Sweat Analysis Using a Portable Device Based on a Screen-printed Electrolyte Sensor. *Electroanalysis* 2018; 30(4): 665-671. doi.org/10.1002/elan.201700672
- [14] Mazzaracchio V, Fiore L, Nappi S, Marrocco G, Arduini F. Medium-distance affordable, flexible and wireless epidermal sensor for pH monitoring in sweat. *Talanta* 2021; 222 121502. doi.org/10.1016/j.talanta.2020.121502
- [15] Zhai Q, Yap LW, Wang R, Gong S, Guo Z, Liu Y, *et al.* Vertically aligned gold nanowires as stretchable and wearable epidermal ion-selective electrode for noninvasive multiplexed sweat analysis. *Analytical chemistry* 2020; 92(6): 4647-4655. doi.org/10.1021/acs.analchem.0c00274
- [16] Huttunen O-H, Happonen T, Hiitola-Keinänen J, Korhonen P, Ollila J. Roll-to-roll screen-printed silver conductors on a polydimethyl siloxane substrate

- for stretchable electronics. *Industrial Engineering Chemistry Research* 2019; 58(43): 19909-19916. doi.org/10.1021/acs.iecr.9b03628
- [17] Liang J, Tong K, Pei Q. A water-based silver-nanowire screen-print ink for the fabrication of stretchable conductors and wearable thin-film transistors. *Advanced Materials* 2016; 28(28): 5986-5996. doi.org/10.1002/adma.201600772
- [18] Kim DS, Jeong J-M, Park HJ, Kim YK, Lee KG. Highly concentrated, conductive, defect-free graphene ink for screen-printed sensor application. *Nano-micro letters* 2021; 13 1-14. doi.org/10.1007/s40820-021-00617-3
- [19] Joshi P, Mishra R, Narayan RJ. Biosensing applications of carbon-based materials. *Current Opinion in Biomedical Engineering* 2021; 18 100274. doi.org/10.1016/j.cobme.2021.100274
- [20] Wang SC, Chang K, Yuan C-J. Enhancement of electrochemical properties of screen-printed carbon electrodes by oxygen plasma treatment. *Electrochimica Acta* 2009; 54(21): 4937-4943. doi.org/10.1016/j.electacta.2009.04.006
- [21] Naqvi STR, Rasheed T, Ashiq MN, ul Haq MN, Majeed S, Fatima B, *et al.* Fabrication of iron modified screen printed carbon electrode for sensing of amino acids. *Polyhedron* 2020; 180 114426. doi.org/10.1016/j.poly.2020.114426
- [22] Rungsawang T, Punrat E, Adkins J, Henry C, Chailapakul O. Development of Electrochemical Paper-based Glucose Sensor Using Cellulose-4-aminophenylboronic Acid-modified Screen-printed Carbon Electrode. *Electroanalysis* 2016; 28(3): 462-468. doi.org/10.1002/elan.201500406
- [23] Kour R, Arya S, Young S-J, Gupta V, Bandhoria P. Recent advances in carbon nanomaterials as electrochemical biosensors. *Journal of The Electrochemical Society* 2020; 167(3): 037555. DOI 10.1149/1945-7111/ab6bc4
- [24] Petroni JM, Lucca BG, Ferreira VS. Simple approach for the fabrication of screen-printed carbon-based electrode for amperometric detection on

- microchip electrophoresis. *Analytica chimica acta* 2017; 954 88-96. doi.org/10.1016/j.aca.2016.12.027
- [25] Guzsvány V, Anojčić J, Radulović E, Vajdle O, Stanković I, Madarász D, *et al.* Screen-printed enzymatic glucose biosensor based on a composite made from multiwalled carbon nanotubes and palladium containing particles. *Microchimica Acta* 2017; 184 1987-1996. doi.org/10.1007/s00604-017-2188-1
- [26] Kumar PA, Pradeep A, Nair BKG, Babu TS, Suneesh PV. Silver-manganese nanocomposite modified screen-printed carbon electrode in the fabrication of an electrochemical, disposable biosensor strip for cystic fibrosis. *Microchimica Acta* 2022; 189(9): 327. doi.org/10.1007/s00604-022-05431-1
- [27] Dai L, Chang DW, Baek JB, Lu W. Carbon nanomaterials for advanced energy conversion and storage. *small* 2012; 8(8): 1130-1166. doi.org/10.1002/sml.201101594
- [28] Yang C, Denno ME, Pyakurel P, Venton BJ. Recent trends in carbon nanomaterial-based electrochemical sensors for biomolecules: A review. *Analytica chimica acta* 2015; 887 17-37. doi.org/10.1016/j.aca.2015.05.049
- [29] Zhang C, Du X. Electrochemical sensors based on carbon nanomaterial used in diagnosing metabolic disease. *Frontiers in Chemistry* 2020; 8 651. doi.org/10.3389/fchem.2020.00651
- [30] Tamirat AG, Guan X, Liu J, Luo J, Xia Y. Redox mediators as charge agents for changing electrochemical reactions. *Chemical Society Reviews* 2020; 49(20): 7454-7478. doi.org/10.1039/D0CS00489H
- [31] Ozoemena KI, Nyokong T. Novel amperometric glucose biosensor based on an ether-linked cobalt (II) phthalocyanine–cobalt (II) tetraphenylporphyrin pentamer as a redox mediator. *Electrochimica Acta* 2006; 51(24): 5131-5136. doi.org/10.1016/j.electacta.2006.03.055

- [32] Ghica ME, Brett CM. A glucose biosensor using methyl viologen redox mediator on carbon film electrodes. *Analytica Chimica Acta* 2005; 532(2): 145-151. doi.org/10.1016/j.aca.2004.10.058
- [33] Xia N, Zhang Y, Wei X, Huang Y, Liu L. An electrochemical microRNAs biosensor with the signal amplification of alkaline phosphatase and electrochemical–chemical–chemical redox cycling. *Analytica Chimica Acta* 2015; 878 95-101. doi.org/10.1016/j.aca.2015.04.018
- [34] Estrada-Osorio D, Escalona-Villalpando RA, Gutiérrez A, Arriaga L, Ledesma-García J. Poly-L-lysine-modified with ferrocene to obtain a redox polymer for mediated glucose biosensor application. *Bioelectrochemistry* 2022; 146 108147. doi.org/10.1016/j.bioelechem.2022.108147
- [35] Gutierrez F, Rubianes MD, Rivas GA. Dispersion of multi-wall carbon nanotubes in glucose oxidase: characterization and analytical applications for glucose biosensing. *Sensors Actuators B: Chemical* 2012; 161(1): 191-197. doi.org/10.1016/j.snb.2011.10.010
- [36] Vasilescu A, Hayat A, Gáspár S, Marty JL. Advantages of carbon nanomaterials in electrochemical aptasensors for food analysis. *Electroanalysis* 2018; 30(1): 2-19. doi.org/10.1002/elan.201700578
- [37] Lu Y-J, Wei K-C, Ma C-CM, Yang S-Y, Chen J-P. Dual targeted delivery of doxorubicin to cancer cells using folate-conjugated magnetic multi-walled carbon nanotubes. *Colloids Surfaces B: Biointerfaces* 2012; 89 1-9. doi.org/10.1016/j.colsurfb.2011.08.001
- [38] Oliveira TM, Morais S. New generation of electrochemical sensors based on multi-walled carbon nanotubes. *Applied Sciences* 2018; 8(10): 1925. doi.org/10.3390/app8101925
- [39] Palumbo A, Li Z, Yang E-H. Trends on carbon nanotube-based flexible and wearable sensors via electrochemical and mechanical stimuli: A review. *IEEE Sensors Journal* 2022. 10.1109/JSEN.2022.3198847

- [40] Zhao Q, Gan Z, Zhuang Q. Electrochemical sensors based on carbon nanotubes. *Electroanalysis: An International Journal Devoted to Fundamental and Practical Aspects of Electroanalysis* 2002; 14(23): 1609-1613. doi.org/10.1002/elan.200290000
- [41] Yu H, Jin Y, Zhan GD, Liang X. Solvent-free solid-state lithium battery based on lifepo4 and mwcnt/peo/pvdf-hfp for high-temperature applications. *ACS omega* 2021; 6(43): 29060-29070. doi.org/10.1021/acsomega.1c04275
- [42] Li Z, Chen S, Nambiar S, Sun Y, Zhang M, Zheng W, *et al.* PMMA/MWCNT nanocomposite for proton radiation shielding applications. *Nanotechnology* 2016; 27(23): 234001. 10.1088/0957-4484/27/23/234001
- [43] Nitin MS, Suresh Kumar S. Ballistic performance of synergistically toughened Kevlar/epoxy composite targets reinforced with multiwalled carbon nanotubes/graphene nanofillers. *Polymer Composites* 2022; 43(2): 782-797. doi.org/10.1002/pc.26409
- [44] Murugan E, Akshata C, Yogaraj V, Sudhandiran G, Babu D. Synthesis, characterization and in vitro evaluation of dendrimer-MWCNT reinforced SrHAP composite for bone tissue engineering. *Ceramics International* 2022; 48(11): 16000-16009. doi.org/10.1016/j.ceramint.2022.02.143
- [45] Karimi-Maleh H, Cellat K, Arıkan K, Savk A, Karimi F. Palladium–Nickel nanoparticles decorated on Functionalized-MWCNT for high precision non-enzymatic glucose sensing. *Materials Chemistry and Physics* 2020; 250 123042. doi.org/10.1016/j.matchemphys.2020.123042
- [46] Mubarak N, Abdullah E, Jayakumar N, Sahu J. An overview on methods for the production of carbon nanotubes. *Journal of Industrial Engineering Chemistry* 2014; 20(4): 1186-1197. doi.org/10.1016/j.jiec.2013.09.001
- [47] Zhao J, Wei L, Peng C, Su Y, Yang Z, Zhang L, *et al.* A non-enzymatic glucose sensor based on the composite of cubic Cu nanoparticles and arc-synthesized multi-walled carbon nanotubes. *Biosensors and bioelectronics* 2013; 47 86-91. doi.org/10.1016/j.bios.2013.02.032

- [48] Ando Y, Zhao X, Sugai T, Kumar M. Growing carbon nanotubes. *Materials today* 2004; 7(10): 22-29. doi.org/10.1016/S1369-7021(04)00446-8
- [49] Nochit P, Sub-udom P, Teepoo S. Multiwalled carbon nanotube (MWCNT) based electrochemical paper-based analytical device (ePAD) for the determination of catechol in wastewater. *Analytical Letters* 2021; 54(15): 2484-2497. doi.org/10.1080/00032719.2021.1872591
- [50] Couto RA, Quinaz MB. Development of a Nafion/MWCNT-SPCE-based portable sensor for the voltammetric analysis of the anti-tuberculosis drug ethambutol. *Sensors* 2016; 16(7): 1015. doi.org/10.3390/s16071015
- [51] Maity D, Minitha C, RT RK. Glucose oxidase immobilized amine terminated multiwall carbon nanotubes/reduced graphene oxide/polyaniline/gold nanoparticles modified screen-printed carbon electrode for highly sensitive amperometric glucose detection. *Materials Science and Engineering: C* 2019; 105 110075. doi.org/10.1016/j.msec.2019.110075
- [52] Zhao Y, Yang X, Pan P, Liu J, Yang Z, Wei J, *et al.* All-printed flexible electrochemical sensor based on polyaniline electronic ink for copper (II), lead (II) and mercury (II) ion determination. *Journal of Electronic Materials* 2020; 49 6695-6705. doi.org/10.1007/s11664-020-08418-x
- [53] Gopi PK, Srinithi S, Chen S-M, Ravikumar CH. Designing of cerium-doped bismuth vanadate nanorods/functionalized-MWCNT nanocomposite for the high toxicity of 4-cyanophenol herbicide detection in human urine sample. *Colloids Surfaces A: Physicochemical Engineering Aspects* 2022; 639 128371. doi.org/10.1016/j.colsurfa.2022.128371
- [54] Altug H, Oh S-H, Maier SA, Homola J. Advances and applications of nanophotonic biosensors. *Nature nanotechnology* 2022; 17(1): 5-16. doi.org/10.1038/s41565-021-01045-5
- [55] Prasanna SB, Sakthivel R, Lin L-Y, Duann Y-F, He J-H, Liu T-Y, *et al.* MOF derived 2D-flake-like structured Mn₃Co₃O₄ integrated acid functionalized MWCNT for electrochemical detection of antibiotic furazolidone in biological

- fluids. *Applied Surface Science* 2023; 611 155784. doi.org/10.1016/j.apsusc.2022.155784
- [56] Wang J, Musameh M. Carbon nanotube screen-printed electrochemical sensors. *Analyst* 2004; 129(1): 1-2. 10.1039/B313431H
- [57] Bucur B, Purcarea C, Andreescu S, Vasilescu A. Addressing the Selectivity of enzyme biosensors: Solutions and perspectives. *Sensors* 2021; 21(9): 3038. doi.org/10.3390/s21093038
- [58] Alvarado-Ramírez L, Rostro-Alanis M, Rodríguez-Rodríguez J, Sosa-Hernández JE, Melchor-Martínez EM, Iqbal HM, *et al.* Enzyme (single and multiple) and nanozyme biosensors: recent developments and their novel applications in the water-food-health nexus. *Biosensors* 2021; 11(11): 410. doi.org/10.3390/bios11110410
- [59] Mokhtar NF, Abd. Rahman RNZR, Muhd Noor ND, Mohd Shariff F, Mohamad Ali MS. The immobilization of lipases on porous support by adsorption and hydrophobic interaction method. *Catalysts* 2020; 10(7): 744. doi.org/10.3390/catal10070744
- [60] Karadurmus L, Kaya SI, Ozkan SA. Recent advances of enzyme biosensors for pesticide detection in foods. *Journal of Food Measurement Characterization* 2021; 15(5): 4582-4595. doi.org/10.1007/s11694-021-01032-3
- [61] Monteiro T, Almeida MG. Electrochemical enzyme biosensors revisited: Old solutions for new problems. *Critical reviews in analytical chemistry* 2019; 49(1): 44-66. doi.org/10.1080/10408347.2018.1461552
- [62] Akhtar MA, Batool R, Hayat A, Han D, Riaz S, Khan SU, *et al.* Functionalized graphene oxide bridging between enzyme and Au-sputtered screen-printed interface for glucose detection. 2019; 2(3): 1589-1596. doi.org/10.1021/acsanm.9b00041
- [63] Amara U, Mahmood K, Riaz S, Nasir M, Hayat A, Hanif M, *et al.* Self-assembled perylene-tetracarboxylic acid/multi-walled carbon nanotube adducts based modification of screen-printed interface for efficient enzyme

immobilization towards glucose biosensing. *Microchemical Journal* 2021; 165 106109. doi.org/10.1016/j.microc.2021.106109

- [64] Bollella P, Gorton L, Ludwig R, Antiochia R. A third generation glucose biosensor based on cellobiose dehydrogenase immobilized on a glassy carbon electrode decorated with electrodeposited gold nanoparticles: Characterization and application in human saliva. *Sensors* 2017; 17(8): 1912. doi.org/10.3390/s17081912
- [65] Mohamad Nor N, Ridhuan NS, Abdul Razak K. Progress of Enzymatic and Non-Enzymatic Electrochemical Glucose Biosensor Based on Nanomaterial-Modified Electrode. *Biosensors* 2022; 12(12): 1136. doi.org/10.3390/bios12121136
- [66] Zhu Z, Garcia-Gancedo L, Flewitt AJ, Xie H, Moussy F. A critical review of glucose biosensors based on carbon nanomaterials: carbon nanotubes and graphene. *Sensors* 2012; 12(5): 5996-6022. doi.org/10.3390/s120505996
- [67] Walton ME, Bouret S. What is the relationship between dopamine and effort? *Trends in neurosciences* 2019; 42(2): 79-91. doi.org/10.1016/j.tins.2018.10.001
- [68] Guo X, Yue H, Song S, Huang S, Gao X, Chen H, *et al.* Simultaneous electrochemical determination of dopamine and uric acid based on MoS₂nanoflowers-graphene/ITO electrode. *Microchemical Journal* 2020; 154 104527. doi.org/10.1016/j.microc.2019.104527
- [69] Sarkar C, Basu B, Chakroborty D, Dasgupta PS, Basu S. The immunoregulatory role of dopamine: an update. *Brain, behavior, and immunity* 2010; 24(4): 525-528. doi.org/10.1016/j.bbi.2009.10.015
- [70] Rubí B, Maechler P. Minireview: new roles for peripheral dopamine on metabolic control and tumor growth: let's seek the balance. *Endocrinology* 2010; 151(12): 5570-5581. doi.org/10.1210/en.2010-0745

- [71] Alm PA. The dopamine system and automatization of movement sequences: a review with relevance for speech and stuttering. *Frontiers in human neuroscience* 2021; 663. doi.org/10.3389/fnhum.2021.661880
- [72] Dalirirad S, Steckl AJ. Lateral flow assay using aptamer-based sensing for on-site detection of dopamine in urine. *Analytical biochemistry* 2020; 596 113637. doi.org/10.1016/j.ab.2020.113637
- [73] Mitchell UH, Obray JD, Hunsaker E, Garcia BT, Clarke TJ, Hope S, *et al.* Peripheral dopamine in restless legs syndrome. *Frontiers in neurology* 2018; 9 155. doi.org/10.3389/fneur.2018.00155
- [74] Ali SR, Ma Y, Parajuli RR, Balogun Y, Lai WY-C. A nonoxidative sensor based on a self-doped polyaniline/carbon nanotube composite for sensitive and selective detection of the neurotransmitter dopamine. *Analytical Chemistry* 2007; 79(6): 2583-2587. doi.org/10.1021/ac062068o
- [75] Santonocito R, Tuccitto N, Pappalardo A, Trusso Sfrassetto G. Smartphone-Based Dopamine Detection by Fluorescent Supramolecular Sensor. *Molecules* 2022; 27(21): 7503. doi.org/10.3390/molecules27217503
- [76] Algov I, Feiertag A, Shikler R, Alfonta L. Sensitive enzymatic determination of neurotransmitters in artificial sweat. *Biosensors and Bioelectronics* 2022; 210 114264. doi.org/10.1016/j.bios.2022.114264
- [77] Tai L-C, Liaw TS, Lin Y, Nyein HY, Bariya M, Ji W, *et al.* Wearable sweat band for noninvasive levodopa monitoring. *Nano letters* 2019; 19(9): 6346-6351. doi.org/10.1021/acs.nanolett.9b02478
- [78] Vázquez-Guardado A, Barkam S, Pepler M, Biswas A, Dennis W, Das S, *et al.* Enzyme-free plasmonic biosensor for direct detection of neurotransmitter dopamine from whole blood. *Nano letters* 2018; 19(1): 449-454. doi.org/10.1021/acs.nanolett.8b04253
- [79] Sajid M, Baig N, Alhooshani K. Chemically modified electrodes for electrochemical detection of dopamine: Challenges and opportunities. *TrAC*

- Trends in Analytical Chemistry 2019; 118 368-385.
doi.org/10.1016/j.trac.2019.05.042
- [80] Ahmad K, Kim H. Design and fabrication of WO₃/SPE for dopamine sensing application. *Materials Chemistry and Physics* 2022; 287 126298. doi.org/10.1016/j.matchemphys.2022.126298
- [81] Tchekep AK, Venkatesan K, Tcheumi H, Suryanarayanan V, Pattanayak DK. Sonochemical fabrication of a hybrid electrode material based on pristine carbon nanotubes and bentonite clay for fast and highly sensitive determination of dopamine in the presence of ascorbic and uric acid. *Materials Chemistry and Physics* 2022; 292 126867. doi.org/10.1016/j.matchemphys.2022.126867
- [82] Dinu LA, Kurbanoglu S, Romanitan C, Pruneanu S, Serban AB, Stoian MC, *et al.* Electrodeposited copper nanocubes on multi-layer graphene: A novel nanozyme for ultrasensitive dopamine detection from biological samples. *Applied Surface Science* 2022; 604 154392. doi.org/10.1016/j.apsusc.2022.154392
- [83] Blankenship RE. *Molecular mechanisms of photosynthesis*, 3rd ed. John Wiley & Sons; 2021.
- [84] Farrow S, Strachan A. *The really useful science book: a framework of knowledge for primary teachers*, 4th ed. Routledge; 2017.
- [85] Korla K, Mitra CK. Modelling the Krebs cycle and oxidative phosphorylation. *Journal of Biomolecular Structure Dynamics* 2014; 32(2): 242-256. doi.org/10.1080/07391102.2012.762723
- [86] Xu XD, Lin BB, Feng J, Wang Y, Cheng SX, Zhang XZ, *et al.* Biological Glucose Metabolism Regulated Peptide Self-Assembly as a Simple Visual Biosensor for Glucose Detection. *Macromolecular rapid communications* 2012; 33(5): 426-431. doi.org/10.1002/marc.201100689
- [87] Savino S, Fraaije MW. The vast repertoire of carbohydrate oxidases: An overview. *Biotechnology Advances* 2021; 51 107634. doi.org/10.1016/j.biotechadv.2020.107634

- [88] Yoo E-H, Lee S-Y. Glucose biosensors: an overview of use in clinical practice. *Sensors* 2010; 10(5): 4558-4576. doi.org/10.3390/s100504558
- [89] Kivimäki M, Batty DG, Steptoe A, Kawachi I. *The Routledge International Handbook of Psychosocial Epidemiology*, 1st ed. Routledge; 2017.
- [90] Cole JB, Florez JC. Genetics of diabetes mellitus and diabetes complications. *Nature reviews nephrology* 2020; 16(7): 377-390. doi.org/10.1038/s41581-020-0278-5
- [91] Malhotra BD. *Biosensors: fundamentals and applications*, 1st ed. Smithers Rapra; 2017.
- [92] Şahin S, Merotra J, Kang J, Trenell M, Catt M. Simultaneous electrochemical detection of glucose and non-esterified fatty acids (NEFAs) for diabetes management. *IEEE Sensors Journal* 2018; 18(22): 9075-9080. 10.1109/JSEN.2018.2870071.
- [93] Branagan D, Breslin CB. Electrochemical detection of glucose at physiological pH using gold nanoparticles deposited on carbon nanotubes. *Sensors Actuators B: Chemical* 2019; 282 490-499. doi.org/10.1016/j.snb.2018.11.089
- [94] Du Y, Zhang X, Liu P, Yu D-G, Ge R. Electrospun nanofiber-based glucose sensors for glucose detection. *Frontiers in Chemistry* 2022; 10. 10.3389/fchem.2022.944428
- [95] Galant A, Kaufman R, Wilson J. Glucose: Detection and analysis. *Food chemistry* 2015; 188 149-160. doi.org/10.1016/j.foodchem.2015.04.071
- [96] Guilbault G. Newer Fluorometric Methods for the Analysis of Biologically Important Compounds. *Journal of Research of the National Bureau of Standards. Section A, Physics* 1972; 76(6): 607. 10.6028/jres.076A.053
- [97] Ling Y, Zhang N, Qu F, Wen T, Gao ZF, Li NB, *et al.* Fluorescent detection of hydrogen peroxide and glucose with polyethyleneimine-templated Cu nanoclusters. *Spectrochimica Acta Part A: Molecular Biomolecular Spectroscopy* 2014; 118 315-320. doi.org/10.1016/j.saa.2013.08.097

- [98] Deigner H-P, Kohl M. Nanoparticles and nanosized structures in diagnostics and therapy, 1st ed. Elsevier Science; 2018.
- [99] Pham X-H, Seong B, Hahm E, Huynh K-H, Kim Y-H, Kim J, *et al.* Glucose detection of 4-mercaptophenylboronic acid-immobilized gold-silver core-shell assembled silica nanostructure by surface enhanced Raman scattering. *Nanomaterials* 2021; 11(4): 948. doi.org/10.3390/nano11040948
- [100] Karim MN, Anderson SR, Singh S, Ramanathan R, Bansal V. Nanostructured silver fabric as a free-standing NanoZyme for colorimetric detection of glucose in urine. *Biosensors and Bioelectronics* 2018; 110 8-15. doi.org/10.1016/j.bios.2018.03.025
- [101] Lindon JC, Tranter GE, Koppenaal DW.(Ed.) *Encyclopedia of Spectroscopy and Spectrometry*, 3rd ed. Elsevier Science; 2017.
- [102] Chen YA, Tsai FJ, Zeng YT, Wang JC, Hong CP, Huang PH, *et al.* Fast and Effective Turn-on Paper-based Phosphorescence Biosensor for Detection of Glucose in Serum. *Journal of the Chinese Chemical Society* 2016; 63(5): 424-431. doi.org/10.1002/jccs.201500488
- [103] Zaidi SA, Shin JH. Recent developments in nanostructure based electrochemical glucose sensors. *Talanta* 2016; 149 30-42. doi.org/10.1016/j.talanta.2015.11.033
- [104] Drake KF, Van Duyne RP, Bond AM. Cyclic differential pulse voltammetry: A versatile instrumental approach using a computerized system. *Journal of Electroanalytical Chemistry Interfacial Electrochemistry* 1978; 89(2): 231-246. doi.org/10.1016/S0022-0728(78)80187-9
- [105] Crespi F. Differential Pulse Voltammetry: Evolution of an In Vivo Methodology and New Chemical Entries, A Short Review. *Journal of New Developments in Chemistry* 2020; 2(4): 20. 10.14302/issn.2377-2549.jndc-20-3298
- [106] Mounesh, Venugopal Reddy K, Fasiulla. Novel tetracinnamide cobalt (II) phthalocyanine immobilized on MWCNTs for amperometric sensing of

- glucose. *Analytical Chemistry Letters* 2020; 10(2): 137-151. doi.org/10.1080/22297928.2020.1760132
- [107] Zou B, Wang P, Yan Y, Mutombo J. Enzyme biosensors systems based on co-modification of carbon nanotubes and enzyme for detection of glucose in food. *Journal of The Electrochemical Society* 2021; 168(6): 065501. 10.1149/1945-7111/ac064d
- [108] Silveira CM, Almeida MG. Small electron-transfer proteins as mediators in enzymatic electrochemical biosensors. *Analytical bioanalytical chemistry* 2013; 405(11): 3619-3635. doi.org/10.1007/s00216-013-6786-4
- [109] El-Desoky HS, Koleeb AI, Bassuiny RI, Mohamed TM. Development of an Effective and Economic Biosensor for Diabetic Blood Monitoring Based on MWCNTs, Artificial Redox Mediator Ferrocene, Nafion Polymer and a Local Extracted and Purified Glucose Oxidase Enzyme from *Penicillium Notatum* F-158 Fungus. *Journal of The Electrochemical Society* 2021; 168(12): 127502. 10.1149/1945-7111/ac3a2b
- [110] Yüzer E, Doğan V, Kılıç V, Şen M. Smartphone embedded deep learning approach for highly accurate and automated colorimetric lactate analysis in sweat. *Sensors Actuators B: Chemical* 2022; 371 132489. doi.org/10.1016/j.snb.2022.132489
- [111] Kisannagar RR, Jha P, Navalkar A, Maji SK, Gupta D. Fabrication of silver nanowire/polydimethylsiloxane dry electrodes by a vacuum filtration method for electrophysiological signal monitoring. *ACS omega* 2020; 5(18): 10260-10265. doi.org/10.1021/acsomega.9b03678
- [112] Kang P-L, Lin Y-H, Settu K, Yen C-S, Yeh C-Y, Liu J-T, *et al.* A facile fabrication of biodegradable and biocompatible cross-linked gelatin as screen printing substrates. *Polymers* 2020; 12(5): 1186. doi.org/10.3390/polym12051186
- [113] Li C, Li Z, Zeng Y, Cao X, Zhao H, Yang YY, *et al.* Co₃O₄ nanowires capable of discharging low voltage electricity showing potent antibacterial activity for

treatment of bacterial skin infection. *Advanced Healthcare Materials* 2022; 11(3): 2102044. doi.org/10.1002/adhm.202102044

- [114] Bujes-Garrido J, Arcos-Martínez M. Development of a wearable electrochemical sensor for voltammetric determination of chloride ions. *Sensors Actuators B: Chemical* 2017; 240: 224-228. doi.org/10.1016/j.snb.2016.08.119
- [115] Simoska O, Duay J, Stevenson KJ. Electrochemical detection of Multianalyte biomarkers in wound healing efficacy. *ACS sensors* 2020; 5(11): 3547-3557. doi.org/10.1021/acssensors.0c01697
- [116] Rajar K, Balouch A, Bhangar M, Shaikh T. Suberic acid functionalized CuO NFs for enhanced electrochemical oxidation of formoterol fumarate. *Sensors Actuators B: Chemical* 2017; 246: 1030-1038. doi.org/10.1016/j.snb.2017.02.111
- [117] Güneş F, Aykaç A, Erol M, Erdem Ç, Hano H, Uzunbayir B, *et al.* Synthesis of hierarchical hetero-composite of graphene foam/ α -Fe₂O₃ nanowires and its application on glucose biosensors. *Journal of Alloys Compounds* 2022; 895: 162688. doi.org/10.1016/j.jallcom.2021.162688
- [118] Pavličková M, Lorencová L, Hatala M, Kováč M, Tkáč J. Facile fabrication of screen-printed MoS₂ electrodes for electrochemical sensing of dopamine. *Scientific Reports* 2022; 12(1): 11900. doi.org/10.1038/s41598-022-16187-2
- [119] Anshori I, Althof RR, Rizalputri LN, Ariasena E, Handayani M, Pradana A, *et al.* Gold Nanospikes Formation on Screen-Printed Carbon Electrode through Electrodeposition Method for Non-enzymatic Electrochemical Sensor. *Metals* 2022; 12(12): 2116. doi.org/10.3390/met12122116
- [120] Arbabi N, Beitollahi H. Ti₃C₂ Nano Layer Modified Screen Printed Electrode as a Highly Sensitive Electrochemical Sensor for the Simultaneous Determination of Dopamine and Tyrosine. *Surface Engineering Applied Electrochemistry* 2022; 58(1): 13-19. doi.org/10.3103/S1068375522010082

- [121] Altun M, Bilgi Kamaç M, Bilgi A, Yılmaz M. Dopamine biosensor based on screen-printed electrode modified with reduced graphene oxide, polynuclear red and gold nanoparticle. *International Journal of Environmental Analytical Chemistry* 2020; 100(4): 451-467. doi.org/10.1080/03067319.2020.1720669
- [122] Mohammadi S, Taher MA, Beitollahi H. Treated screen printed electrodes based on electrochemically reduced graphene nanoribbons for the sensitive voltammetric determination of dopamine in the presence of uric acid. *Electroanalysis* 2020; 32(9): 2036-2044. doi.org/10.1002/elan.201900767
- [123] Settu K, Huang Y-M, Zhou S-X. A facile approach for the electrochemical sensing of dopamine using paper-based PEDOT: PSS/RGO graphene biosensor. *ECS Journal of Solid State Science Technology* 2020; 9(12): 121002. 10.1149/2162-8777/abca28
- [124] Baccarin M, Rowley-Neale SJ, Cavalheiro ÉT, Smith GC, Banks CE. Nanodiamond based surface modified screen-printed electrodes for the simultaneous voltammetric determination of dopamine and uric acid. *Microchimica Acta* 2019; 186 1-9. doi.org/10.1007/s00604-019-3315-y
- [125] Selvolini G, Lazzarini C, Marrazza G. Electrochemical nanocomposite single-use sensor for dopamine detection. *Sensors* 2019; 19(14): 3097. doi.org/10.3390/s19143097
- [126] Şen M, Azizi E, Avcı İ, Aykaç A, Ensarioğlu K, Ok İ, *et al.* Screen printed carbon electrodes modified with 3D nanostructured materials for bioanalysis. *Electroanalysis* 2022; 34(9): 1463-1471. doi.org/10.1002/elan.202100624
- [127] Tavella F, Ampelli C, Leonardi SG, Neri G. Photo-electrochemical sensing of dopamine by a novel porous TiO₂ array-modified screen-printed Ti electrode. *Sensors* 2018; 18(10): 3566. doi.org/10.3390/s18103566
- [128] Brouzgou A, Gorbova E, Wang Y, Jing S, Seretis A, Liang Z, *et al.* Nitrogen-doped 3D hierarchical ordered mesoporous carbon supported palladium electrocatalyst for the simultaneous detection of ascorbic acid, dopamine, and glucose. *Ionics* 2019; 25 6061-6070. doi.org/10.1007/s11581-019-03116-z

- [129] Lee H, Hong YJ, Baik S, Hyeon T, Kim DH. Enzyme-based glucose sensor: from invasive to wearable device. *Advanced healthcare materials* 2018; 7(8): 1701150. doi.org/10.1002/adhm.201701150
- [130] Moyer J, Wilson D, Finkelshtein I, Wong B, Potts R. Correlation between sweat glucose and blood glucose in subjects with diabetes. *Diabetes technology and therapeutics* 2012; 14(5): 398-402. doi.org/10.1089/dia.2011.0262
- [131] Zheng L, Liu Y, Zhang C. A sample-to-answer, wearable cloth-based electrochemical sensor (WCECS) for point-of-care detection of glucose in sweat. *Sensors and Actuators B: Chemical* 2021; 343 130131. doi.org/10.1016/j.snb.2021.130131
- [132] Phasukom K, Sirivat A. Chronoampermetric detection of enzymatic glucose sensor based on doped polyindole/MWCNT composites modified onto screen-printed carbon electrode as portable sensing device for diabetes. *RSC advances* 2022; 12(44): 28505-28518. 10.1039/D2RA04947C
- [133] Onur Uygun Z, Ertuğrul Uygun HD. A Novel Chronoimpedimetric Glucose Sensor in Real Blood Samples Modified by Glucose-imprinted Pyrrole-Aminophenylboronic Acid Modified Screen Printed Electrode. *Electroanalysis* 2020; 32(2): 226-229. doi.org/10.1002/elan.201900537
- [134] Sadak O. One-pot scalable synthesis of rGO/AuNPs nanocomposite and its application in enzymatic glucose biosensor. *Nanocomposites* 2021; 7(1): 44-52. doi.org/10.1080/20550324.2021.1917837
- [135] Cai Y, Liang B, Chen S, Zhu Q, Tu T, Wu K, *et al.* One-step modification of nano-polyaniline/glucose oxidase on double-side printed flexible electrode for continuous glucose monitoring: Characterization, cytotoxicity evaluation and in vivo experiment. *Biosensors and Bioelectronics* 2020; 165 112408. doi.org/10.1016/j.bios.2020.112408
- [136] Sakdaphetsiri K, Teanphonkrang S, Schulte A. Cheap and Sustainable Biosensor Fabrication by Enzyme Immobilization in Commercial Polyacrylic

Acid/Carbon Nanotube Films. ACS omega 2022; 7(23): 19347-19354.
doi.org/10.1021/acsomega.2c00925

- [137] Phetsang S, Jakmunee J, Mungkornasawakul P, Laocharoensuk R, Ounnunkad K. Sensitive amperometric biosensors for detection of glucose and cholesterol using a platinum/reduced graphene oxide/poly (3-aminobenzoic acid) film-modified screen-printed carbon electrode. Bioelectrochemistry 2019; 127 125-135. doi.org/10.1016/j.bioelechem.2019.01.008
- [138] Sun Y, Ma J, Wang Y, Qiao S, Feng Y, Li Z, *et al.* A Wearable Patch Sensor for Simultaneous Detection of Dopamine and Glucose in Sweat. Analytica 2023; 4(2): 170-181. doi.org/10.3390/analytica4020014
- [139] Ramírez-Sánchez K, Alvarado-Hidalgo F, Zamora-Sequeira R, Sáenz-Arce G, Rojas-Carrillo O, Avedaño-Soto E, *et al.* Biosensor based on the directly enzyme immobilization into a gold nanotriangles/conductive polymer biocompatible coat for electrochemical detection of Chlorpyrifos in water. Medical Devices and Sensors 2019; 2(5-6): e10047. doi.org/10.1002/mds3.10047
- [140] Nichols SP, Koh A, Storm WL, Shin JH, Schoenfisch MH. Biocompatible materials for continuous glucose monitoring devices. Chemical reviews 2013; 113(4): 2528-2549. doi.org/10.1021/cr300387j

Appendices

Appendix A

Publications from the Thesis

Journal Articles

1. İpek AVCI, Merve OĞUZ & Mustafa ŞEN. (2021). Detection of pH and Urea with an Extended Gate Field-Effect Transistor Based Microsensor. *Avrupa Bilim ve Teknoloji Dergisi*, (31), 874-880.

Projects

1. Production, Characterization and Application of Cost-Effective Screen-Printed Flexible and Inflexible Electrodes with Nano-Carbon-Based Conductive Unique Paste Formulations (Supplied by TUBITAK 1005) (April 2023-Present) (Project No: 222M400).

2. Development of Multi-Walled Carbon Nanotube-Based Flexible Screen-Printed Disposable Electrodes for Sensor Applications. (Supplied by TUBITAK 2210/C-Domestic Priority Areas Graduate Scholarship Program) (October 2021-September 2022) (Application No: 1649B022111832).

Curriculum Vitae

Name Surname : Merve Oğuz

Education:

2015–2020 Bachelor of Science, İzmir Kâtip Çelebi University, Dept. of Biomedical Eng.

2020–Present Bachelor of Science, Anadolu University (Open Course), Dept. of Management of IT Systems

2021–Present Master of Science, İzmir Kâtip Çelebi University, Dept. of Biomedical Eng.

Publications:

1. Oğuz, M., Aykaç, A., & Şen, M. (2023). Highly Sensitive and Selective Electrochemical Detection of Dopamine and Uric Acid Using Sea Urchin-like Tungsten Oxide Nanostructure Modified SPCE.
2. İpek AVCI, Merve OĞUZ & Mustafa ŞEN. (2021). Detection of pH and Urea with an Extended Gate Field-Effect Transistor Based Microsensor. *Avrupa Bilim ve Teknoloji Dergisi*, (31), 874-880.
3. Oğuz, M., Avcı, İ., & Mustafa, Ş. E. N. (2021, November). An Extended Gate Field Effect Transistor-based (EGFET-based) Urea Microbiosensor Based on Polypyrrole. In *2021 Medical Technologies Congress (TIPTEKNO)* (pp. 1-4). IEEE.
4. AVCI, Ipek; OĞUZ, Merve; ŞEN, Mustafa. An Extended Gate Field Effect Transistor (EGFET) pH Microsensor. In: *2021 Medical Technologies Congress (TIPTEKNO)*. IEEE, 2021. p. 1-3.

Projects:

- Production, Characterization and Application of Cost-Effective Screen-Printed Flexible and Inflexible Electrodes with Nano-Carbon-Based Conductive Unique Paste Formulations (Supplied by TUBITAK 1005) (April 2023-Present) (Project No: 222M400).
- Development of Multi-Walled Carbon Nanotube-Based Flexible Screen-Printed Disposable Electrodes for Sensor Applications. (Supplied by TUBITAK 2210/C- Domestic Priority Areas Graduate Scholarship Program) (October 2021-September 2022) (Application No: 1649B022111832).

Certifications and Courses:

- KOSGEB: Traditional Entrepreneurship Course (continues)
- Introduction to Information Technology (2023)
- ISO 13485:2016 Biomedical Device Quality Management (2019)
- ISO / IEC 17025:2017 Qualification of Testing and Calibration of Laboratories (2019)
- ISO 15189:2012 Medical Laboratories Requirements for Quality and Competence (2019)
- ISO 9001:2015 Quality Management System (2019)